COMPLEX GLYCAN SYNTHESIS IN BACTERIA

by

Timothy William Wallen

A thesis submitted to the faculty of
The University of North Carolina at Charlotte
in partial fulfillment of the requirements
for the degree of Master of Science in
Chemistry

Charlotte

2019

Approved by:

_____
Dr. Jerry Troutman

_____
Dr. Brian Cooper

_____
Dr. Juan Vivero-Escoto

_____
Dr. Yuri Nesmelov

ABSTRACT

TIMOTHY WILLIAM WALLEN. Complex glycan synthesis in bacteria. (Under the direction of DR. JERRY TROUTMAN)

Glycans, which are assembled through a process known as glycosylation, are critical for creating biological structures important for the function and vitality of bacterial cells. In order to study the synthesis of glycans, enzymes and intermediates involved in the various pathways are studied using analytical tools such as fluorescent isoprenoid probes as well as liquid chromatography-mass spectrometry (LC-MS) analysis. The research here focuses on an *in vitro* analysis of WecG, WecB, and WecC involved in the production of Enterobacterial common antigen (ECA) as well as glycolipid intermediates in the *H. pylori* biosynthetic pathway. UDP-ManNAcA, a substrate used by WecG, is not commercially available, so enzymatic synthesis has been attempted in the Troutman Lab utilizing two other ECA enzymes, WecB (an epimerase) and WecC (a dehydrogenase) with confirmation of activity through detection of UDP-N-acetylhexosaminuronic acid (HexNAcA) sugars by the development of a novel LC-MS method utilizing the properties of a Hydrophilic Interaction Liquid Chromatography-Zwitterionic (HILIC-Z) column for separation and detection of highly polar compounds. Through this method, it has been observed that WecC can produce UDP-GlcNAcA as well, a novel finding that has also resulted in difficulties in obtaining UDP-ManNAcA. This unexpected finding has led to probing WecC for specificity as well as a kinetic analysis. WecG's activity as a N-acetyl-D-mannosaminuronic acid (ManNAcA) transferase has been successfully verified *in vitro* and is being probed for specificity.

Proteins have begun to be expressed for studying the *H. pylori* glycosylation pathway and this research is currently in its nascent stages.

TABLE OF CONTENTS

LIST OF TABLES

LIST OF FIGURES

LIST OF ABBREVIATIONS

2CN-BP	2-cyanoanilino bactoprenyl monophosphate
2CNA	2-nitrileanilinogeranyl
2CNA-GPP	2-nitrileanilinogeranyl pyrophosphate
B. cereus	*Bacillus cereus*
B. longum	*Bifidobacterium longum*
BLUSP	UDP-Sugar pyrophosphorylase
BPP	bactoprenyl diphosphate
BP	bactoprenyl phosphate
bp	base pairs
B. subtilis	*Bacillus subtilis*
C_{55}	55-cis isoprene additions
CPSA	Capsular Polysaccharide A
ECA	enterobacterial common antigen
E. coli	*Escherichia coli*
ESI-MS	electrospray ionization – mass spectrometry
Fuc4NAc	4*N*-acetylfucosamine
FPP	farnesyl diphosphate
FPLC	fast protein liquid chromatography
Gal	galactose
GalNAc	*N*-acetylgalactosamine
Glc	glucose
GlcA	glucuronic acid

GlcNAc	*N*-acetylglucosamine
GlcNAcA	*N*-acetylglucosaminuronic acid
GC-MS	gas chromatography - mass spectrometry
HexNAcA	N-acetylhexosaminuronic acid
H. pylori	*Helicobacter pylori*
HILIC-Z	hydrophilic interaction liquid chromatography - zwitterionic
HPLC	high performance liquid chromatography
IPP	isopentenyl diphosphate
IPTG	isopropyl β-D-1-thiogalactopyranoside
kDa	kilodaltons
K_m	Michaelis constant
LB	lysogeny broth
LC-MS	liquid chromatography - mass spectrometry
LIC	ligation independent cloning
MOE	metabolic oligosaccharide engineering
$ManN_3$	mannosazide
ManNAc	N-acetylmannosamine
ManNAcA	N-acetylmannosaminuronic acid
$ManNH_2$	mannosamine
M. maripaludis	*Methanococcus maripaludis*
NAD	nicotinamide adenine dinucleotide
NahK	a kinase
N-linked	nitrogen linked

Ni-NTA	nickel nitrilotriacetic acid
NH_2	a primary amine
NMR	nuclear magnetic resonance
O-linked	oxygen linked
PCR	polymerase chain reaction
PGT	phospho glycosyltransferase
PMBN	polymyxin B nonapeptide
RCF	relative centrifugal force
RffH	a transferase
RmlB	a dehydratase
S. aureus	*Staphylococcus aureus*
SEC	Size Exclusion Chromatography
UDP	uridine diphosphate
UPPS	undecaprenyl pyrophosphate synthase
UV	ultraviolet
Δ*wecA*	A *wecA* deletion mutant
WecA	an initiating phospho glycosyltransferase
WecB	an epimerase
WecC	a dehydrogenase
WecD	an acetyltransferase
WecE	a transaminase
WecF	a Fuc4NAc transferase
WecG	a ManNAcA transferase

CHAPTER 1: INTRODUCTION

1.1 The importance of glycoscience and the study of glycan synthesis

Glycoscience is the study of glycans (a polymerized sugar also known as polysaccharides, oligosaccharides, or carbohydrates) which are the most abundant organic molecule family and are macromolecules critical for the function and vitality of cells. If the pathways that produce glycans are disrupted, the organism ceases to function. An interest in studying these pathways in bacteria has arisen due to the drive to discover targets for therapeutics as well as vaccines that are effective against various pathogens. Being made of sugar building blocks, glycan structures can exist as linear or branched with a level of complexity not found in nucleic acids or proteins (Fig. 1.).[1] This is due to the fact that sugars can have various points of linkages and stereochemistries, unlike nucleic acids and proteins that exist primarily in linear forms.

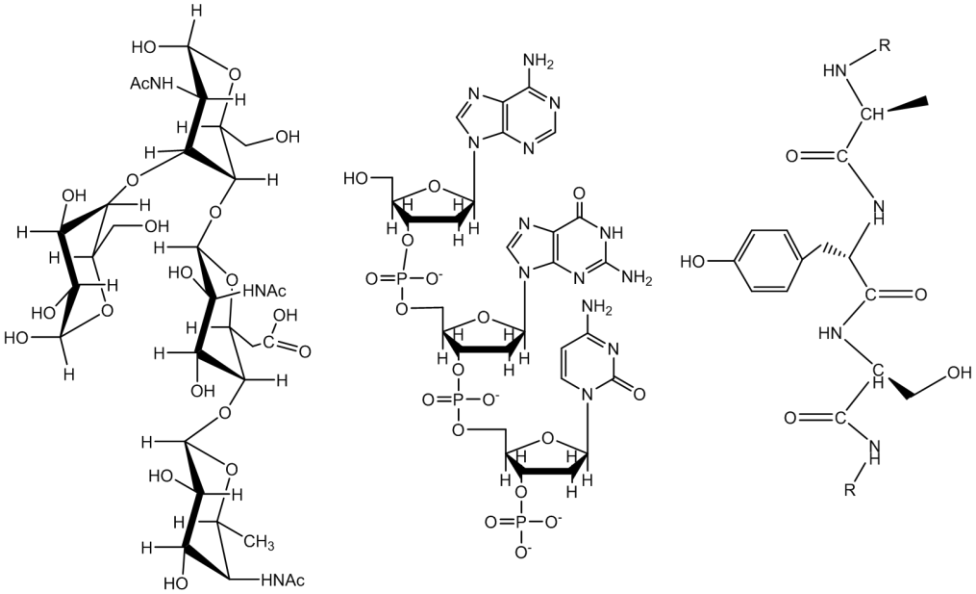

Figure 1. (Left to Right) Structures of glycans, nucleotides, and proteins. Complex truncations and varying stereochemistries can exist in chains of glycans.

A variety of structures with essential functions can be made from glycans including deoxyribose, which is critical for the synthesis of DNA, and polysaccharides that provide structural support for cell walls. In addition, bacteria are encapsulated in various polysaccharides that make up structures such as antigens. In the example of gram negative bacteria, this “capsule” rests on the outer membrane, peptidoglycan that resides in the periplasm, and an inner membrane made up of a phospholipid bilayer (Fig. 2).[2] An integral part of all of these layers, glycans can also be bound to other macromolecules to create structures known as glycoconjugates such as glycolipids (glycan + lipid) and glycoproteins (glycan + protein). These products are synthesized through biosynthetic glycosylation pathways, with glycoproteins assembled through either a covalent oxygen linkage (O-linked) or nitrogen linkage (N-linked) to amino acid residues on the protein.[3]

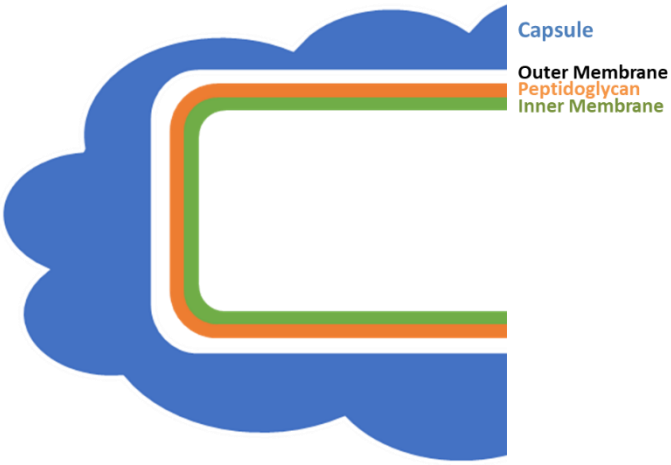

Figure 2. Encapsulated *E. coli* cross-section. The capsule is on top of the outer membrane in which many polysaccharide structures are found.

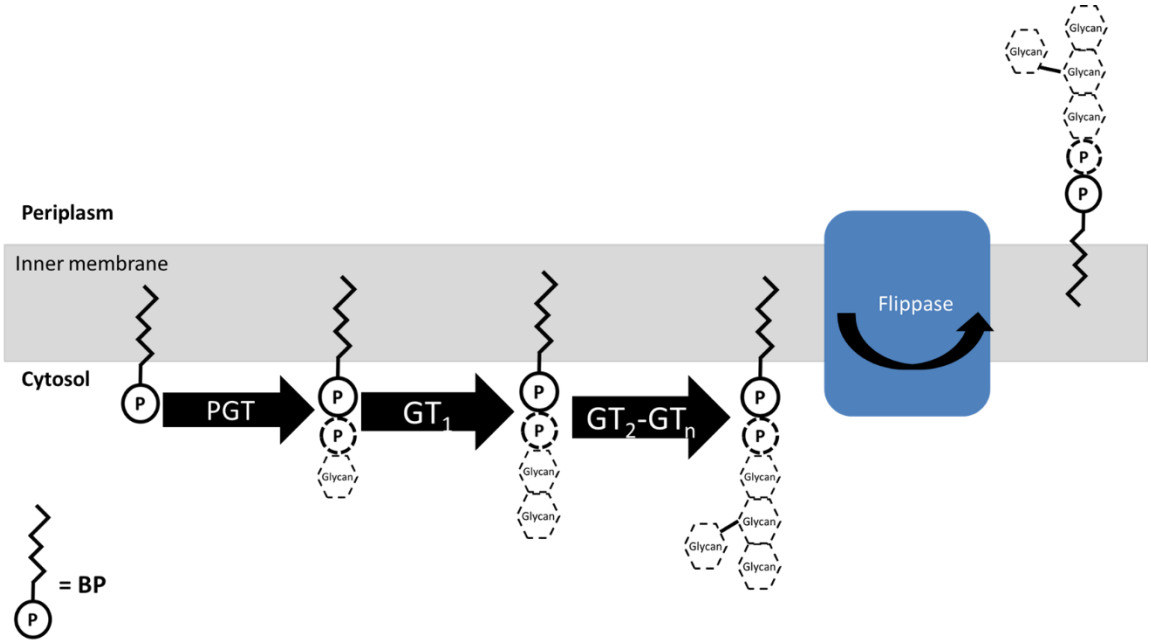

Figure 3. General schematic of lipid carrier-mediated glycosylation. A PGT transfers a sugar phosphate and subsequent glycosyl transferases ($GT_{1\text{-}n}$) attach sugars until the completed unit is transported to the periplasm through a flippase.

Glycoconjugates are built stepwise inside the cell in the cytosol and are commonly produced through a lipid carrier-mediated pathway (Fig. 3).[2] In the lipid carrier-mediated assembly pathway a C_{55} polyisoprenoid lipid derivative, bactoprenyl phosphate (BP), acts as an anchor on the inner membrane of the cell and a sugar phosphate is appended by an initiating phosphoglycosyltransferase (PGT) with subsequent sugar residues attached by glycosyltransferases. The completed structure is then transported outside the cell via a flippase. If the final product is a glycoprotein, the final polysaccharide is covalently attached to a protein. In glycosylation pathways, glycosyltransferases earlier in the pathway should yield shorter, simpler glycans while those later in the pathway will produce complex branched structures. Due to the variety of intermediates and enzymes involved in these glycosylation pathways there is an inherent complexity that requires effective analytical tools for successful study. The

research described here investigates the Enterobacterial Common Antigen and *H. pylori* glycosylation pathways.

1.2 The Enterobacterial Common Antigen (ECA) Pathway

The Enterobacterial common antigen (ECA) pathway is of particular importance as it is found in every member of the large Enterobacteriaceae family including pathogens such as *Salmonella*, *Escherichia*, *Yersinia*, *Klebsiella*, and *Shigella*. The ECA pathway is a biosynthetic pathway that is responsible for synthesis of a capsular polysaccharide found on the surface of these bacteria. Three forms of the ECA are known to exist in bacteria: ECA_{PG} (a phosphoglyceride ECA anchored to the cell surface), ECA_{CYC} (4-6 trisaccharide units found in a cyclic form found in the periplasm of the cell), and ECA_{LPS} (with the antigen polysaccharide covalently bound to a lipopolysaccharide, a glycolipid found on the surface of the cell) with ECA_{PG} being the most common.[4] All of these are composed of a repeating trisaccharide (or three sugar molecule) of →1)-α-d- N-acetylglucosamine(GlcNAc)-(4→1)-β-d- N-acetyl-

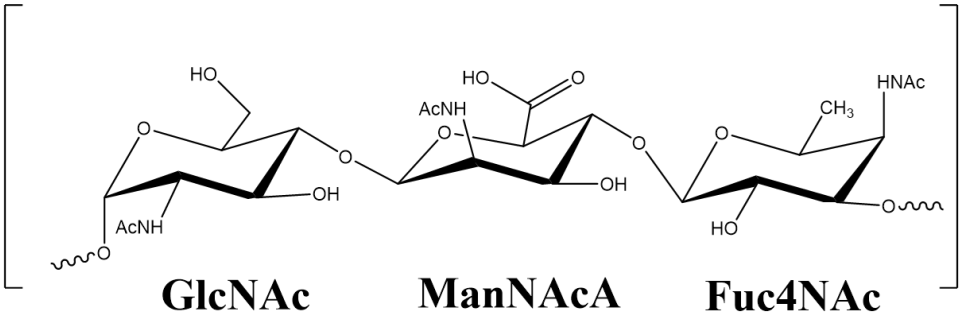

Figure 4. ECA trisaccharide (GlcNAc-ManNAcA-Fuc4NAc) repeating units found on gram negative bacteria

mannosaminuronic acid(ManNAcA)-(4 →1)-α-d- 4-acetamido-2,4-dideoxygalactose(Fuc4NAc)-(3→ (Fig. 4).This repeating unit has been confirmed in isolated ECA from cell lysates by characterization with nuclear magnetic resonance

(NMR) by Basu et al. in *Plesiomonas shigelloids*, *Salmonaella montevido*, and *Shigella sonnei* (1987).[5] ECA has also been characterized in *Escherichia coli* through NMR and electrospray ionization mass spectrometry (ESI-MS) by Erbel et al. (2003).[4] The specific functions of the enzymes involved in the synthesis of ECA have been previously identified by Barr et al. through *in vitro* synthesis by incubating deletion mutants with radiolabeled nucleotide sugars with verification by gel-permeation chromatography (1989).[6]

The ECA is assembled by first WecA, an initiating phosphoglycsoyltransferase, transferring a phosphate GlcNAc onto a BP lipid anchor to give a BPP-GlcNAc to produce the first lipid-sugar intermediate (Fig. 5). WecG is a ManNAcA transferase that yields the two sugar intermediate BPP-GlcNAc-ManNAcA utilizing the substrate UDP-

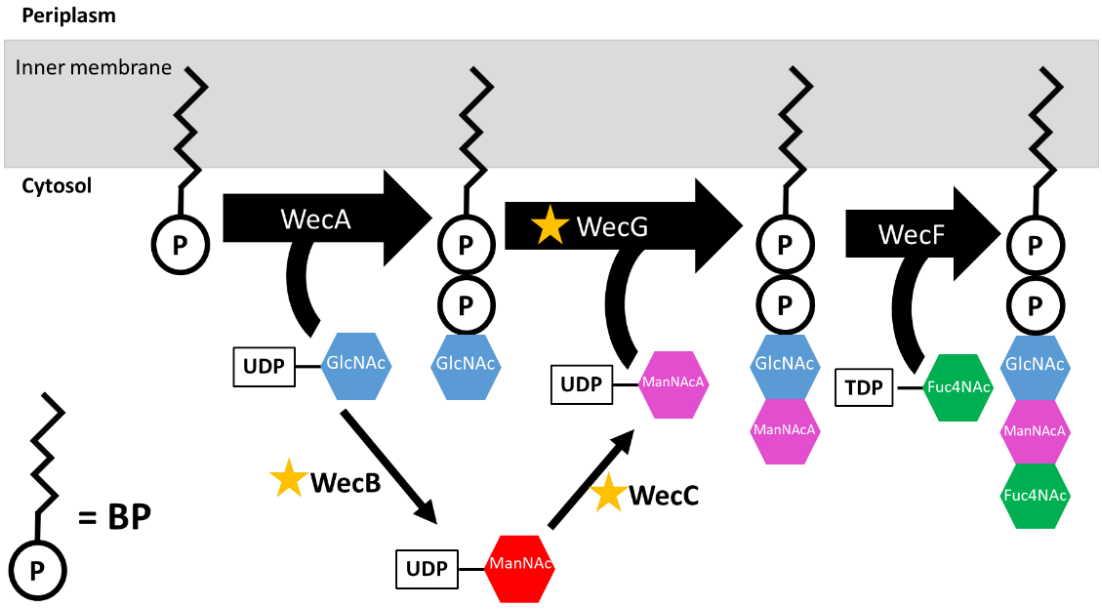

Figure 5. The ECA Pathway. WecG (transferase), WecB (epimerase), and WecC (dehydrogenase) will be focused on through *in vitro* work.

ManNAcA which is made from UDP-GlcNAc being converted by WecB and WecC.

Finally WecF transfers Fuc4NAc from TDP-Fuc4NAc to give the completed common antigen product BPP-GlcNAc-ManNAcA-Fuc4NAc. Here the ECA pathway will be studied *in vitro* through the analysis of WecG, WecB, and WecC.

1.3 *Helicobacter pylori* glycosylation pathway

H. pylori is a gastric pathogen known to cause a variety of gastrointestinal diseases. For *H. pylori* to infect a host's stomach, these bacteria require motility in the form of flagella, which are built from glycoproteins.[7] The glycosyltransferases involved in the production of these structures remain targets of interest for therapeutics. Literature suggests that glycosylation occurs in *H. pylori* through an O-linked and N-linked system in the production of lipopolysaccharide precursors to flagellin.[8] Metabolic oligosaccharide engineering (MOE) has been used to metabolically label glycans with an azide bearing sugar acting as a chemical reporter to identify glycosyltransferases.[8] Champasa et al. have identified 125 glycosyltransferases in *H. pylori*; however, which pathways they are involved in remains unknown (2013). [7]

1.4 WecG *in vitro* Analysis

The *wecG* gene encodes for the N-acetyl-D-mannosaminuronic acid (ManNAcA) transferase thought to catalyze the addition of ManNAcA onto the wecA product, BPP-GlcNac, the first intermediate in the ECA pathway.[9] 2-nitrileanilinogeranyl-bactoprenyl phosphate (2CNA-BP) probes (Fig. 6) will help to confirm WecG's *in vitro* activity and probe for potential new polysaccharide products produced by WecG. Evidence of this activity has been

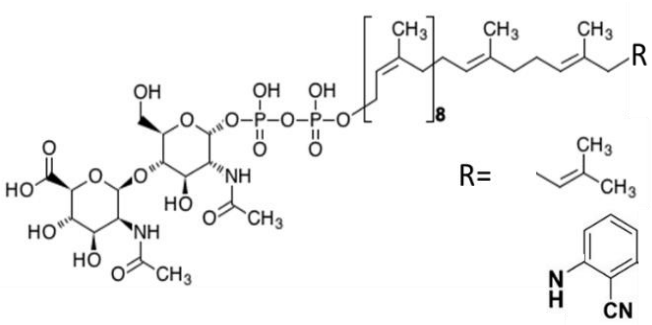

Figure 6. BPP-GlcNac-ManNAcA plus 2CNA fluorescent analogue

obtained by Barr et al. using radioactive glycans *in vitro* with cell membranes of deletion mutants and verified through gel-permeation chromatography[6] but no work has been done with purified WecG.

1.5 Enzymatic Synthesis of UDP-ManNAcA

In order to verify the activity of WecG, UDP-ManNAcA, a commercially unavailable type of UDP N-acetylhexosaminuronic acid (UDP-HexNAcA) sugar, needs

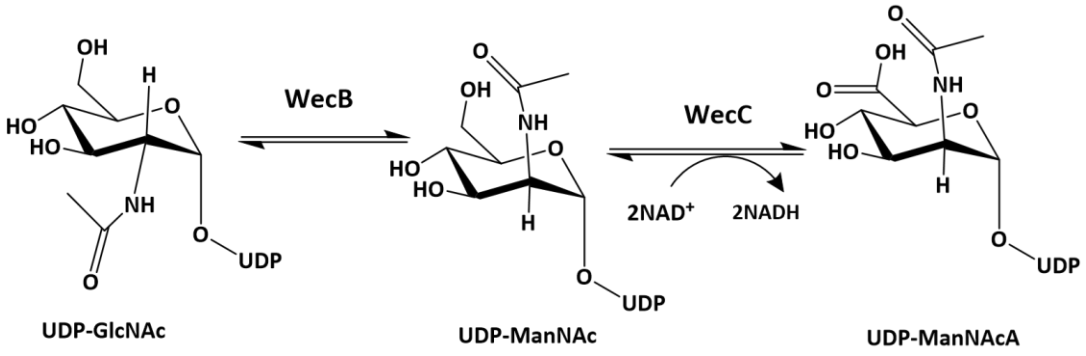

Figure 7. UDP-ManNAcA reaction. WecB (epimerase) converts UDP-GlcNAc to UDP-ManNAc followed by WecC (dehydrogenase) producing UDP-ManNAcA utilizing 2 equivalents of NAD^+ in a redox reaction.

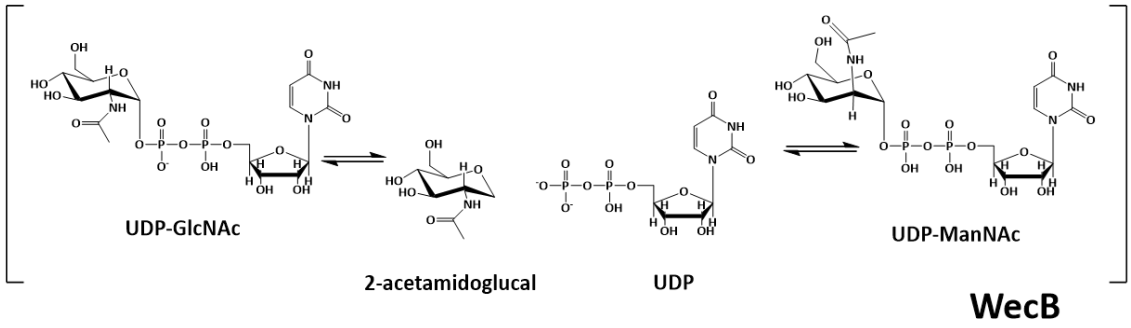

Figure 8. Mechanism of WecB. A *trans*-eliminaton occurs of UDP followed by a *syn*-addition of 2-acetamidoglucal.

to be utilized as a substrate. UDP-ManNAcA is produced by starting with the conversion of UDP-GlcNAc to UDP-ManNAc by the epimerase WecB (Fig.7). This epimerase has been documented to convert UDP-GlcNAc to UDP-ManNAc poorly in a ratio ranging from 9:1 - 12:1 UDP-GlcNA: UDP-ManNAc at equilibrium *in vitro* from gram positive *B. cereus* and *B. subtilis* as well as gram negative *E. coli*.[10,11,12] Sala et al. has proposed

that the mechanism occurs through a *trans*-elimination of the UDP resulting in 2 acetamidoglucal and UDP followed by a *syn*-addition of 2-acetamidoglucal to form UDP-ManNAc (1996) (Fig. 8).[12] The dehydrogenase WecC utilizes 2 equivalents of NAD+ in a redox reaction to oxidize the primary alcohol to give UDP-ManNAcA. Kawamura et al. were able to perform an enzymatic synthesis of UDP-ManNAcA in *E. coli* (1979).[13] WecB was first incubated with UDP-GlcNAc, boiling the reaction to quench it and separating/purifying the UDP-ManNAc product with TLC. UDP-ManNAc was then incubated with WecC and NAD^+ to produce UDP-ManNAcA which was also purified through TLC. Kawamura et al. also showed that it was possible to produce UDP-ManNAcA through a coupled reaction with WecB and WecC in a one pot reaction as WecC did not utilize UDP-GlcNAc as a substrate to produce UDP *N*-acetylglucosaminuronic acid (UDP-GlcNAcA) (1975).[14] WecC's substrate specificity has also been confirmed in homologues found in *M. maripaludis* and *S. aureus*.[15, 16]

In order to verify the activity of the WecB-WecC coupled reaction and UDP-ManNAcA is being produced in *E. coli*, paper chromatography has been used which is time consuming and less precise than modern detection methods. Portoles et al. has used gas chromatography-mass spectrometry (GC-MS) to characterize these enzymes and confirm the production in UDP-ManNAcA in *S. aureus*, but not in *E. coli*.[16]

1.6 Analytical tools for studying glycan products

In order to probe for enzyme activity, radiolabeled sugar nucleotides have been used in the past with separation of unreacted donors from labeled products through techniques such as thin layer chromatography (TLC), high performance liquid chromatography (HPLC), and ion exchange chromatography.[17] Radiolabeling is a highly sensitive method and if the reaction is properly quenched it can be useful for quantitative

kinetic studies, however there are safety concerns when working with radiolabeled compounds as well as experimental design limiting the throughput of such a method. The research discussed here uses fluorescent probes for studying transferases that interact with BP-linked sugar substrates as well as absorbance and LC-MS detection for the confirmation of the synthesis of UDP-sugar substrates. The enzymatic synthesis of lipid anchor BPs first begins through the production of BPP through undecaprenyl pyrophosphate synthase (UPPS), and is assembled by elongating farnesyl diphosphate (FPP), a common isoprenoid biosynthesis intermediate with 3 isoprene units, with eight

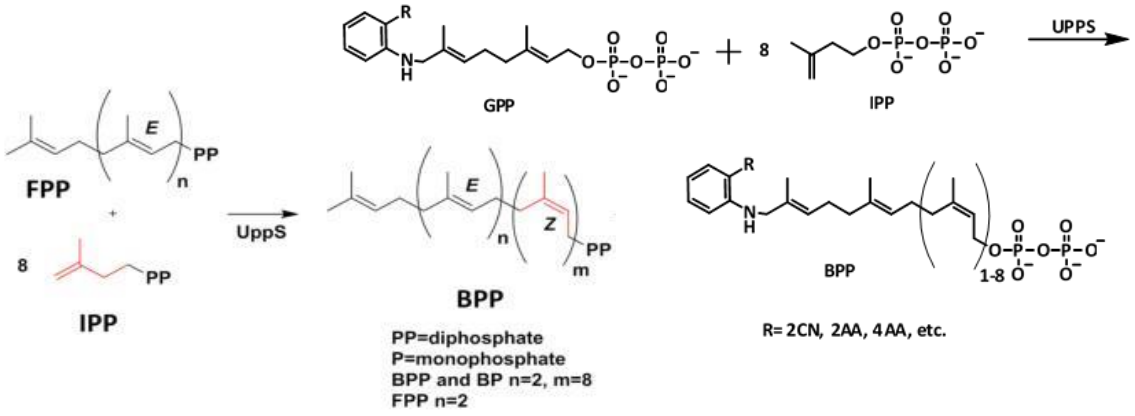

Figure 9. (Left to right) Structure/synthesis of BPP and Fluorescent bactoprenyl production procedure (Troutman et al., 2015)[18]

isopentenyl diphosphates (IPP) that add eight cis-isoprene units to FPP (Fig. 9).[18] A phosphatase then dephosphorylates the BPP by leaving a BP that an initiating phosphoglycosyltransferase can attach a sugar to. By using a 2-nitrileanilinogeranyl (2CNA) analogue of an isoprenoid precursor such as 2-nitrileanilinogeranyl pyrophosphate (2CNA-GPP), fluorescent BPPs can be assembled from which BP-anchors can be built (Fig. 9).[18] For *in vitro* level work in this project, the BPs are used as a fluorescent lipid anchor that can be attached to sugars to analyze the formation of products via HPLC with fluorescence detection which is highly sensitive eliminating the

need for radiolabeling. The 2CNA-BP has a specific retention time and unique fluorescence signature. If a sugar is transferred successfully by a transferase of interest to the anchor and a product is formed, a retention shift and change in fluorescence can be monitored. This method has been successfully applied before in Dr. Troutman's laboratory to monitor the synthesis of Capsular Polysaccharide A (CPSA) in *Bacteroides fragilis* and colonic acid in *Eschericia coli* through *in vitro* means.[19, 20]

In order to verify the synthesis of UDP-sugars, absorbance detection and LC-MS can be used. UDP-Sugars can be detected on an HPLC with UV detector by measuring the retention time of UDP-sugars at 260 nm giving a chromatogram which reveals separation of initial substrates and products. UDP-sugars are inherently difficult to separate due their high polarity and charge. Thus the choice of HPLC column and appropriate conditions have to take the structure of UDP-sugars into consideration. Using normal-phase can result in very long retention times and reverse-phase columns have issues with separation of UDP-sugars as the compounds can be so highly charged they will not interact with the column.[21]

In the Troutman lab, an NH_2 column has been used with acidic buffer conditions to separate UDP-sugars. By using high concentrations of acidic buffer a column that normally operates as a reverse-phase column can have a positively

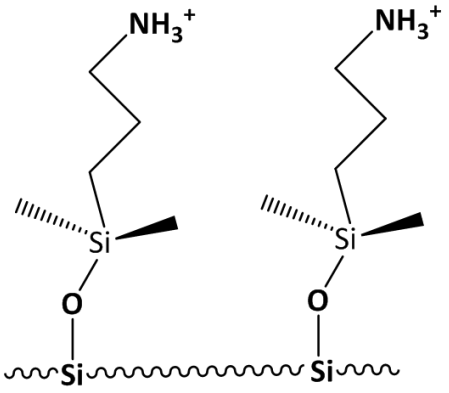

Figure 10. NH_2 column in acidic conditions

charged NH^{3+} functional group that allows for negatively charged UDP sugars to stick on the column (Fig. 10). A limitation with this method is that LC-MS electrospray ionization (ESI) cannot be used in tandem due to the high concentrations of buffer salts.[21]

In order to employ in line LC-MS detection, a hydrophilic interaction liquid chromatography-zwitterionic (HILIC-Z) column has been used which utilizes a zwitterionic functional group bonded onto a silica stationary phase which exists as a zwitterion in the operable pH range of the column (Fig. 11).[22] Warth et al. have employed this technique recently for analysis of nucleotide sugars in wheat extracts showing successful separation of UDP-glucose (Glc) and its derivative UDP-Glucuronic acid (GlcA) (2015) but has not been used for *in vitro* analysis of glycosylation pathways. [21] The HILIC-Z column works by separating compounds by hydrophilicity and by charge, and is incredibly effective at doing so with low concentrations of buffer salts allowing for an ideal column for LC-MS method development. By utilizing such analytical tools, the *H. pylori* and ECA glycosylation pathways can be studied.

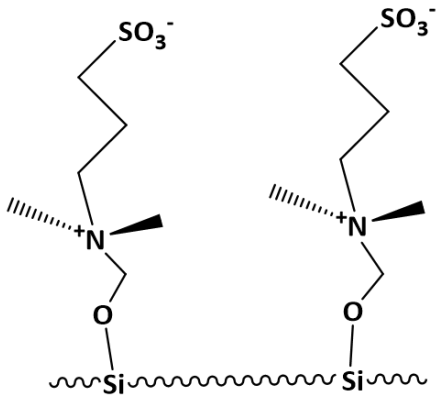

Figure 11. Zwitterionic functional group bound on to silica

1.7 Summary

The synthesis of glycan products is a complex process that requires specialized tools to study. The production of the ECA and *H. pylori* lipopolysaccharide products occur through glycosylation. For glycosylation involving lipid anchors, the Troutman lab has employed fluorescent isoprenoid probes to mimic naturally occurring BP-anchors that are glycan assembly points. The objective of this research is to study both the ECA and

H. pylori pathways. For the ECA pathway, the activity of WecG is studied through the use of established 2CNA-BP probes. A LC-MS method will be developed to study the activity of WecB and WecC as well as detection of UDP-HexNAcA sugars. The *H. pylori* pathway is unknown, so this is exploratory work on the *in vitro* level beginning with the acquisition of glycosyltransferases. In order to probe for the activity of glycosyltransferases and verification of intermediates, fluorescent 2CNA-BP probes will be utilized in a collaboration with Dr. Danielle Dube of Bowdoin College.

CHAPTER 2: MATERIALS AND METHODS

2.1 Cloning of *wecG* transferase

wecG was replicated through polymerase chain reaction (PCR) and the insert was ligated into a pET-24a(+) vector utilizing BamH1 and Xho1 restriction enzymes. The plasmid was then transformed into competent DH5α cells and sent for Sanger sequencing to verify sequence incorporation. A glycerol stock was prepared from DH5α cells, from which purified plasmid with gene inserts were isolated to transform into bacterial strain C41 for protein expression.

2.2 Expression of ECA enzymes

WecB, WecC, and WecG 5mL starter cultures of lysogeny broth (LB) with 50 µg/mL kanamycin from C41 glycerol stocks were prepared and grown for 16 hours at 37°C with shaking. These starter cultures were then diluted 1:100 into 1 L of LB broth with 50 µg/mL kanamycin and grown at 37°C with shaking until the OD_{600} reached 0.5-0.8.

WecB and WecC were both induced with 1 mM of IPTG at 30°C for 8 hours. After IPTG induction, cells were centrifuged at 5,000 relative centrifugal force (RCF) for 15 minutes at 4°C. The supernatant was discarded and the pellet was suspended in 20 mL of lysis buffer (50 mM Tris, pH 8, 20 mM imidazole, 200 mM sodium chloride) and sonicated for 3 minutes. Lysed cells were then spun under vacuum using a Beckman ultracentrifuge at 83,000 RCF for 60 minutes at 4°C. The pellet was discarded and the supernatant was run through a nickel nitrilotriacetic acid (Ni-NTA) column to purify. The flow through (FT), wash (W), and six elutions (E1-E6) were collected in Eppendorf tubes. SDS page was performed to verify in which elutions the proteins were in. Instead

of proceeding with dialysis, purified protein elutions for WecB and WecC were injected onto a fast protein liquid chromatography (FPLC) and were purified using size exclusion chromatography (SEC) through the use of a HiLoad™ 16/60 Superdex™ 200 column and detected at 280 nm. For SEC, 1x dialysis buffer (50 mM Tris-base, 200 mM NaCl in DI H_2O) was run at 1.5 mL/min with a pressure limit of 0.5 MPa for 140 mL total. 3 mL fractionations were collected between 70 and 120 mL. The following protein standards were run to characterize the size and form of WecB and WecC: Blue Dextran (2,000 kDA), Cytochrome C (12.3 kDA), Carbonic Anhydride (29 kDA), Albumin (66 kDA), Alcohol Dehydrogenase (ROHDH) (150 kDA) and Amylase (200 kDA). The fractionations were combined, aliquoted and the concentrations were determined on a NanoDrop spectrophotometer at 280 nm before being stored at -80°C.

WecG was induced with 1 mM IPTG for 4 hours at 37° C. After IPTG induction, cells were centrifuged at 5,000 RCF for 15 minutes at 4°C. The supernatant was discarded and the pellet was suspended in 20 mL of lysis buffer and sonicated for 3 minutes. Lysed cells were then spun under vacuum using a Beckman ultracentrifuge at 83,000 RCF for 60 minutes at 4°C. The pellet was discarded and the supernatant was run through a nickel nitrilotriacetic acid (Ni-NTA) column to purify. The flow through (FT), wash (W), and six elutions (E1-E6) were collected in Eppendorf tubes. SDS page was performed to verify in which elutions the proteins were in and these were combined and pipetted into dialysis tubing to perform dialysis. Dialysis was performed in 1x dialysis buffer, with the dialysis buffer replaced 3 times over the course of dialysis. The first dialysis buffer was gently spun overnight, with subsequent dialysis buffer changes spun for 3-4 hours each time at 4°C. The proteins were then pipetted out of the dialysis tubing

and aliquoted into Eppendorf tubes and stored at -80°C. The concentration of the protein was determined using a Nano Drop spectrophotometer at 280 nm.

2.3 Development of LC-MS method for detection of UDP-ManNAcA

To detect changes in reactions, an Agilent Zorbax NH_2 4.6x150 mm 5µm column was used initally with absorbance detection at 260 nm. The following conditions were used: 125 mM ammonium acetate (pH 4.5) at a flow of 1.00 mL/min for 25 minutes. A standard with 2 mM NAD^+, 1 mM UDP-GlcNAc, and 2 mM NADH standard was prepared by diluting in H_2O and the retention time was checked on the HPLC.

A LC-MS method was also developed and compared to the NH_2 column method utilizing an Agilent Poroshell 120 HILIC-Z 4.6 x 50 mm 2.7 µm column. 1 mM UDP-GlcNAc, 1 mM UDP-Glc, 1 mM UDP-GlcA, 2 mM NAD^+, and 2 mM NADH standards were prepared and used to determine sucessful separation by HPLC and LC-MS detection. Solvents A (10 mM ammonium acetate (pH 9.0) in acetonitrile (ACN)) and B (10 mM ammonium acetate (pH 9.0)) were used. The following conditions were used for initial scouting of reaction substrates: Initial conditions of 95% A and 5% B held for 2 minutes with increasing the concentration of B to 50% over 10 minutes followed by an equilibriation period of 8 minutes with initial conditions (95% A, 5% B) at a flow rate of 0.5 mL/min. Ammonium acetate pH 4.5 and 6.3 were tested as well using the same conditions. The reaction of WecB by itself was observed using a shallow gradient of 80-75% A over 10 minutes. The reaction coupled with WecC was also observed using a gradient of 80-68% A over 10 minutes. For LC-MS detection a Thermo MSQ+ was used in negative ESI mode under 72 psi of nitrogen (N_2) with the following conditions: ion spray voltage -50 V, with probe temp 350°C, and scan mode set to 1.00 second.

2.4 Activity testing of coupled WecB-WecC reaction components

The following general reaction conditions were used to enzymatically synthesize UDP-ManNAcA:100 mM Tris-HCl Buffer (pH 9.0), 2 mM NAD^+, 1 mM UDP-GlcNAc, 20 mM DTT, 3.83 µM WecB, 3 µM WecC in H_2O for overnight at 37°C . Pure UDP-ManNAc (0.9 mM) was given as a gift by Dr. Xi Chen of UC-Davis for some preliminary testing. This standard was used to confirm the formation of UDP-ManNAc in the WecB reaction as well as used with WecC to produce UDP-ManNAcA for testing with WecG.

The activity of the coupled reaction of WecB and WecC was compared to the reaction with just WecC. The substrate specificity of WecC without WecB was tested with 1mM UDP-Glc, UDP-Gal, and UDP-GalNAc as well as 2 mM $NADP^+$ in place of NAD+. Some conditions were also tested to see if they had any effect on the turnover to UDP-HexNAcA including pH, [NAD^+], and [UDP-GlcNAc]. For pH, 100 mM Tris-HCl buffer pH 8.0 and 8.5 were tested as well for activity.

To test the effect of [NAD^+], all other conditions were held constant and the following concentrations were tested: 0 mM, 0.16 mM, 0.5 mM, 1 mM, 2mM, 4.5 mM, and 9 mM of NAD^+. To test the effect of [UDP-GlcNAc], all other conditions were held constant and the following concentrations were tested: 0.25 mM, 0.5 mM, 0.75 mM and 1 mM of UDP-GlcNAc.

2.5 Activity testing of WecC reaction and comparison to coupled WecB-WecC reactions

In order to determine where maximum UDP-HexNAcA was formed during the reaction, aliquots were taken out and quenched by diluting in mobile phase for LC-MS (10 mM Ammonium Acetate pH 9.0 in Acetonitrile (ACN)) for a final dilution of 5% sample to 95% mobile phase at 0.5, 1, 2, and 3 hours at 37°C. The concentration of

WecC was also tested at 3 µM and 1.5 µM. Coupled reactions were also tested with 20 µM WecB and concentrations of WecC at 3, 1.5, and 0.75 µM.

Kinetics were also tested on WecC through timepoints utilizing a Spectramax M5 spectrophotometer and an opaque flat bottomed 384 well plate for kinetic fluorescence assays with the following setting: excitation at 340 nm and emission at 460 nm. The following general reaction conditions were used for the kinetics assay: 100 mM Tris-HCl pH 9.0, 20 mM DTT, 0.8 mM NAD^+, and 0.75 µM of WecC with varying UDP-GlcNAc concentration to a total volume of 25 µL. The following NADH concentrations were used to create a calibration curve in order to convert relative fluorescence units (RFU) to mM NADH formed: 0, 0.1, 0.2, 0.4, 0.6, and 0.8 mM in 100 mM Tris-Hcl pH 9.0 buffer. The following concentrations of UDP-GlcNAc were monitored: 0, 0.4, 0.8, 0.95, 1.5, 3.0, 12, 24, 31, and 47 mM. The activity of the coupled WecB-WecC reaction was monitored using the same general reaction conditions along with 3 µM of WecB and varying the UDP-GlcNAc concentration. The following concentrations of UDP-GlcNAc were monitored: 0, 0.4, 0.8, 0.95, 1.5, 3.0, 8, and 12 mM. Activity of the coupled WecB-WecC reaction was also monitored using the same general reaction conditions but increasing the concentration of NAD^+ to 2 mM and activity at the following UDP-GlcNAc concentrations: 1, 3, 5, 8, and 12 mM. The plate reader was set to 37°C for incubation temperature and the WecB and WecC enzymes were pre-incubated at 37°C for five minutes before addition to reactions. 10 second time points of the reactions were taken over the course of 1 hour.

2.6 Specificity testing of WecG

To test the activity of WecG the following general reaction conditions were utilized: 1 mM of UDP-Sugar, 100 mM Bicine buffer (pH 8.0), 2 mM NAD+, 20 mM DTT, 15 mM sodium cholate, and 20 µM 2CNc4BPP-GlcNAc, 3µM of WecG in H_2O for 1 hour at 37°C. To probe how WecG interacts with the components of the UDP-ManNAcA reaction WecG was tested with substrate 1 mM UDP-GlcNAc along with 3.83 uM WecB and 7.74 uM WecC. Reactions for a control were also run with only WecG, only UDP-GlcNAc, WecG with UDP-GlcNAc and WecB, and WecG with UDP-GlcNAc and WecC. WecG was also tested with an aliquot of UDP-ManNAc and WecC reaction as a UDP-sugar substrate.

WecG was also tested with the following UDP-sugars (all 1 mM concentration): UDP-Glc, UDP-GlcA, UDP-Gal, UDP-GalNAc, GDP-Man, GDP-Fuc4NAc. 2CN-c4-BPP-Gal and 2CN-c4-BPP-Glc were also used to test the effect of changing the 2CN-c4-BPP sugar substrate. All reactions were monitored by the HPLC using fluorescence detection (excitation of 340 nm and emission of 390 nm) on a reverse-phase C18 column with the following conditions: 47% PrOH 53% ammonium bicarbonate for 10 minutes at 1 mL/minute.

2.7 Cloning of *H. pylori* genes

In order to study the glycosyltransferases important in the *H. pylori* biosynthetic pathway, the genes that encode for these enzymes were identified through preliminary work done by Dr. Dube. Dr. Dube created mutants with genes knocked out based on reading frame position in the Helicobacter pylori genome and then metabolic oligosaccharide engineering (MOE) was used to screen for glycoprotein production activity to then identify 13 genes of interest. Six of these genes

(Hp_G27_94,580,613,761,785, and 1509) were already successfully cloned in pBlusescript II (+) vectors by the Dube lab and were sent to the Troutman lab in purified

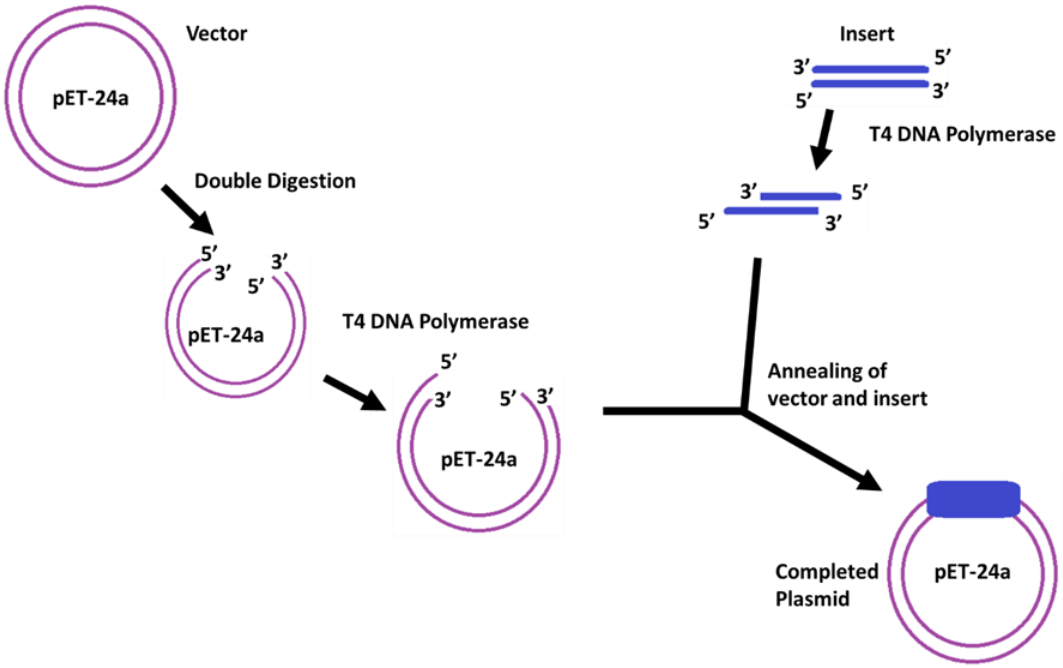

Figure 12. LIC cloning workflow. pET-24a is shown as the vector in this example. Long overhangs are made on both vector and insert with T4 DNA polymerase before finally being annealed.

plasmid form. Since seven genes were left to clone (Hp_G27_190, 579, 607, 645, 952, 1236, and 1518), the approach of ligation independent (LIC) cloning was used in order to increase throughput relative to traditional cloning (Fig. 12). These genes were replicated through polymerase chain reaction (PCR) and the inserts were annealed into a pET-24a (+)-LIC vector after long overhangs were created with T4 DNA polyemerase.[12] These plasmids were then transformed into competent DH5α cells and sent for Sanger sequencing to verify sequence incorporation. Glycerol stocks were prepared from DH5α cells, from which purified plasmid of the genes could be isolated to transform into bacterial strain C41 for protein expression.

2.8 Expression of *H. pylori* membrane fraction (MF) glycosyltransferases

Hp_G27_1518 was transformed into a C41 strain and expression was continued. TMHMM was used to analyze predicted protein membrane domains to determine 1518 was likely found in the membrane. 5mL starter cultures of lysogeny broth (LB) with 50 µg/mL kanamycin from C41 glycerol stocks were prepared and grown for 16 hours at 37°C at 220 RCF on a shaker. This starter cultures was then diluted 1:100 into 1 L of LB broth with 50 µg/mL kanamycin and grown at 37°C with shaking until the OD_{600} reached 0.5-0.8.

Hp_G27_1518 was induced with 1 mM IPTG at 16°C overnight. After IPTG induction cells were centrifuged at 5,000 RCF for 15 minutes at 4°C. The supernatant was discarded and the pellet was suspended in 20 mL of lysis buffer and sonicated for 3 minutes. The lysate was spun at 2,500 RCF for 30 minutes at 4°C. The supernatant containing the membrane fraction (MF) was then spun under vacuum using a Beckman ultracentrifuge at 83,000 RCF for 60 minutes at 4°C. The supernatant was discarded and the pellet was then taken up in ~ 2-3 mL of 1x dialysis buffer and homogenized until a uniform solution was obtained. This solution was aliquoted and stored at -80°C and the concentration was determined utilizing a Bradford Assay.

2.9 Expression of *H. pylori* soluble glycosyltransferases

Hp_G27_190 was transformed into a C41 strain and expression was continued. TMHMM was used to analyze predicted protein membrane domains to determine 190 was likely soluble. A 5 mL starter culture of lysogeny broth (LB) with 50 µg/mL kanamycin from a C41 glycerol stock was prepared and grown for 16 hours at 37°C at 220 RCF on a shaker. This starter culture was then diluted 1:100 into 1 L of LB broth

with 50 µg/mL kanamycin and grown at 37°C at 220 RCF until the OD_{600} reached 0.5-0.8.

Hp_G27_190 was induced with 1 mM IPTG at 34°C for 4 hours. After IPTG induction, cells were centrifuged at 5,000 rcf for 15 minutes at 4°C. The supernatant was discarded and the pellet was suspended in 20 mL of lysis buffer and sonicated for 3 minutes.

Lysed cells were then spun under vacuum using a Beckman ultracentrifuge at 30,000 rcf for 60 minutes at 4°C. The pellet was discarded and the supernatant was run through a nickel nitrilotriacetic acid (Ni-NTA) column to purify. The flow through (FT), wash (W), and six elutions (E1-E6) were collected in Eppendorf tubes. SDS page was performed to verify in which elutions the proteins were in and these were combined and pipetted into dialysis tubing to perform dialysis. Dialysis was performed in 1x dialysis buffer, with the dialysis buffer replaced 3 times over the course of dialysis. The first dialysis buffer was gently spun overnight, with subsequent dialysis buffer changes spun for 3-4 hours each time at 4°C. The proteins were then pipetted out of the dialysis tubing and aliquoted into Eppendorf tubes and stored at -80°C. The concentration of the protein was determined using a Nano Drop spectrophotometer at 280 nm.

CHAPTER 3: RESULTS AND DISCUSSION

3.1 *in vitro* ECA analysis

3.1.1 Cloning and expression of ECA enzymes

In order to study the WecB, WecC and WecG *in* vitro, the genes needed to be cloned into plasmids for protein expression to be able to use in analytical assays. Cloning and sequencing of *wecB and wecC* had already been previously done in the Troutman lab, so only *wecG* was cloned using traditional cloning methods (Fig. 13). WecB, WecC,

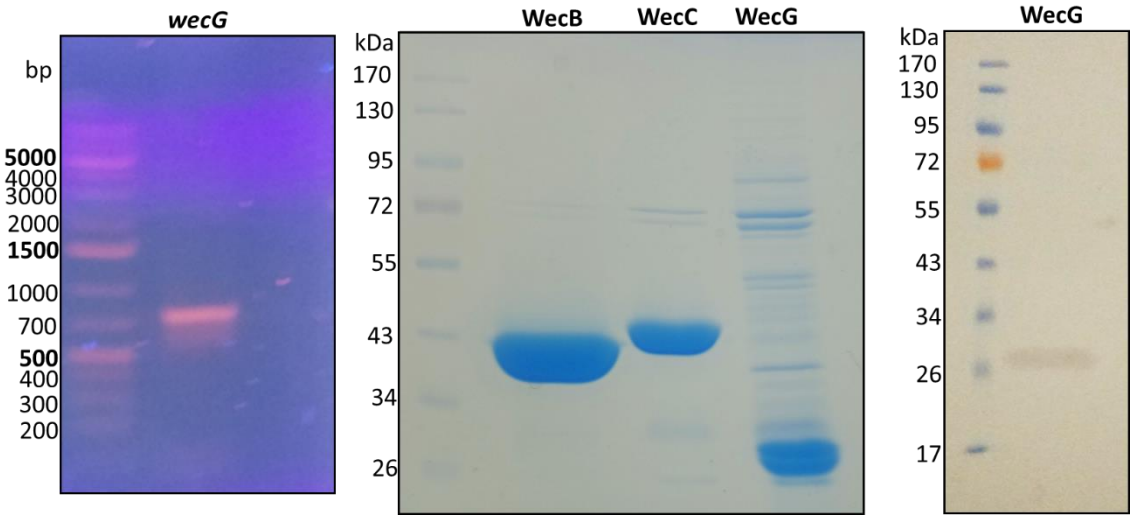

Figure 13. (Left to right) *wecG* PCR analysis with *wecG* appropriate gene size (741 base pairs), SDS-PAGE analysis of WecB, WecC, and WecG expressions, and T7-tag Western Blot analysis of WecG IPTG expression.

and WecG were all expressed successfully as shown in Fig. 13. Since WecG had not been expressed before in the Troutman lab, the protein was verified through the use of a T7-tag western blot (Fig. 13). This antibody T7 tag is encoded in the pET24-a vector, so when the protein is expressed the protein has a T7 tag which can be visualized and confirmed on a western blot through interaction with a secondary antibody.

The sizes and concentrations of expressed proteins are shown in table 1. SEC was performed on WecB and WecC in order to improve the consistency of their enzymatic activity to increase the replicability of UDP-ManNAcA synthesis discussed in section 3.1.3. Purification through SEC could explain why the concentration was much smaller due to diluted sample when collecting fractions.

Table 1. ECA proteins and their concentrations after successful expression. WecB and WecC were purified through SEC resulting in the much lower concentrations

Protein	Molecular Weight (kDa)	Concentration (µM)
WecB	42	12.78
WecC	45	9.38
WecG	28	62.14

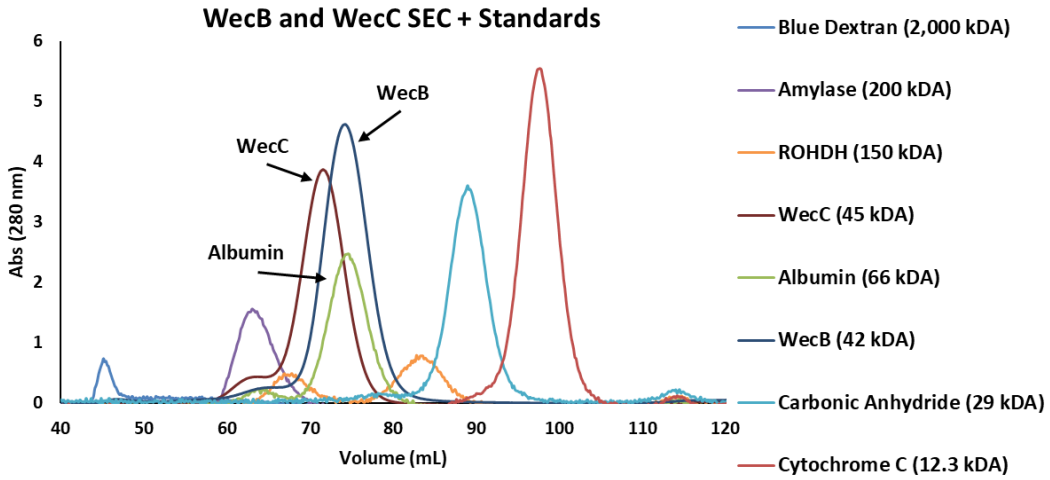

Figure 14. Comparison of WecB and WecC with standards through SEC analysis. WecB and WecC chromatograms were normalized by dividing their original signal by a factor of 25.

In order to understand the structure of WecB and WecC proteins, protein standards were analyzed by SEC and a comparison was made (Fig. 14). WecB and WecC were eluted closest to albumin which is 66 kDA, a dimeric protein, which suggests that

these proteins are dimeric in form as monomeric forms of both of these enzymes would elute before Albumin.

The retention factor of WecB and WecC were also compared to the standards by subtracting the volume and dividing by the flow through standard (Blue Dextran) which was then plotted against molecular weight (Fig. 15). There is a clear correlation between retention factor and size of protein for the standards.

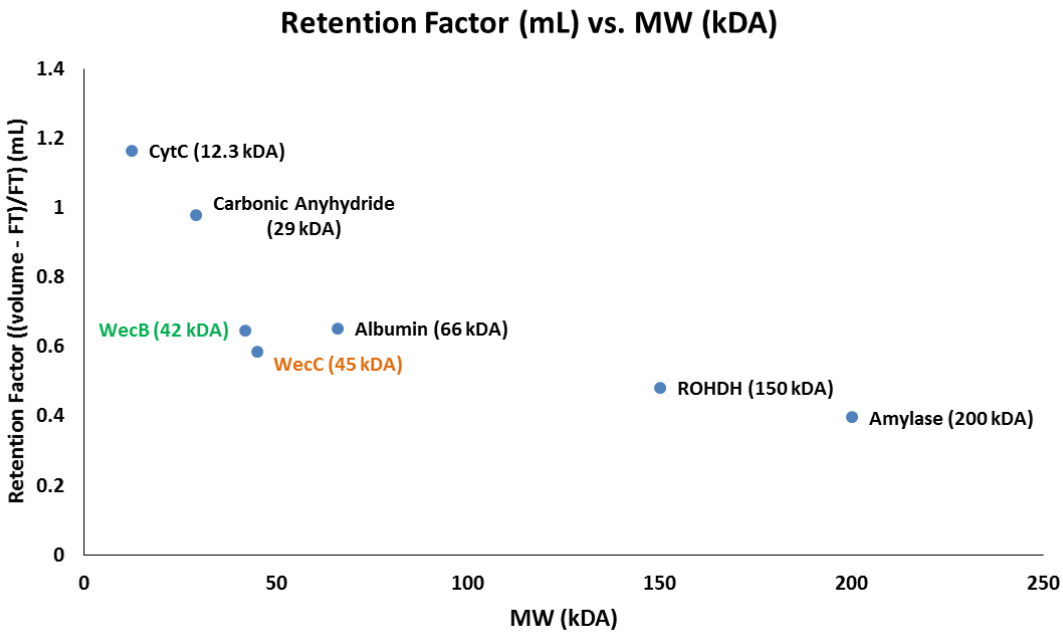

Figure 15. Retention factor ((volume - FT)/FT) plotted against molecular weight of proteins. WecB and WecC have a similar retention factor to Albumin which is similar in molecular weight.

3.1.2 LC-MS method development

A variety of methods were tested to find an optimal method for the separation and detection of a UDP-HexNAcA sugar. Initial screening with the NH_2 column found clear

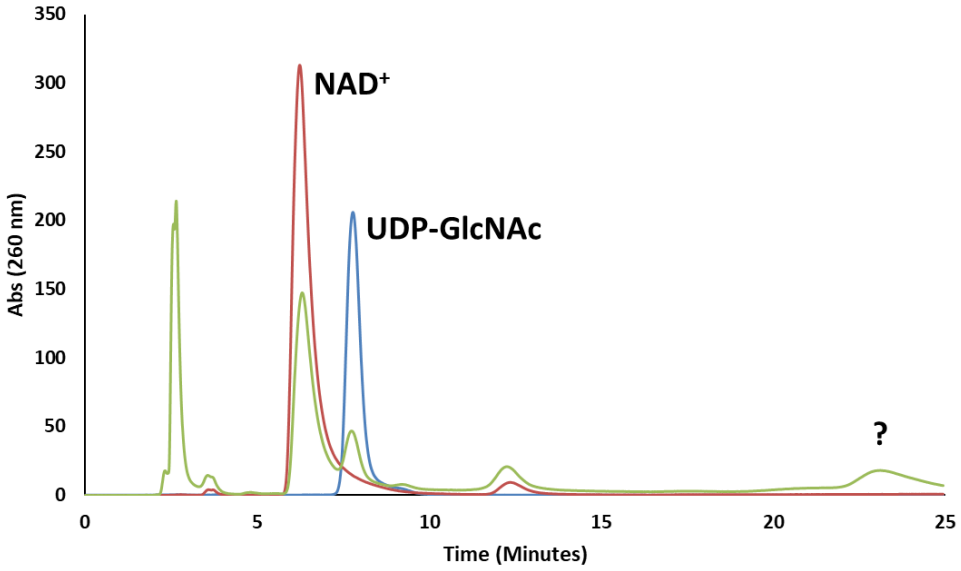

Figure 16. Detection of NAD+ standard (red), UDP-GlcNAc standard (blue), and coupled WecB-WecC reaction (green) on NH_2 column. A small peak at ~13 minutes appears to be found in the NAD+ standard and reaction that is attributed to a potential contaminant in the source of NAD+. A new peak of interest was found at ~23 minutes in the coupled WecB-WecC reaction.

separation of UDP-GlcNAc and NAD+ standards. When injecting a coupled WecB-WecC reaction on the NH_2 column a new peak was observed at approximately 23 minutes (Fig. 16).

The product associated with this peak was collected and subjected to MS analysis on the MSQ+ for mass identification and found to have a mass of 664.09 m/z. In negative ion mode UDP-ManNAcA+ $2Na^+$ ($[M-3H+2Na]^-$, 664.02 m/z) could explain this mass value as the commercially bought UDP-GlcNAc from Sigma-Aldrich is a sodium salt and could exist in the reaction solution. However, NADH ($[M-H]^-$) also has a similar mass (664.12 m/z_ and so an NADH standard was compared on the MSQ+ while also injected on the NH_2 column. A match for the mass was found as well as a retention time match of

25 minutes on the HPLC (Fig. 17). When injecting the NADH standard on the NH_2 column, it was found that it matched the chromatogram of the coupled reaction indicating that NADH was formed. The peak for UDP-GlcNAc was disappearing as it was being consumed but there was no product peak being detected. From these results it was deduced that the formation of NADH was being observed and that UDP-ManNAcA cannot be detected on this column using these conditions. Previous work using this column in the Troutman lab has shown difficulty in detecting UDP-GlcA standard, so a

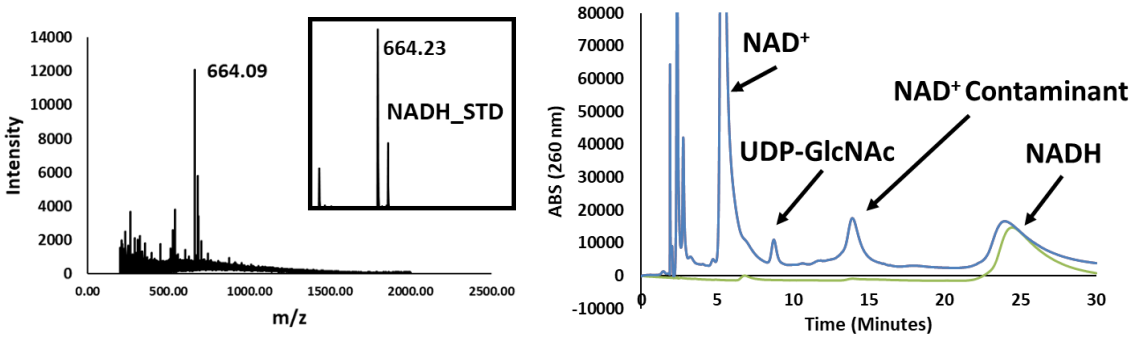

Figure 17. (Left) Mass of isolated fractionation of product peak compared with NADH standard (insert). (Right) Comparison of coupled WecB-WecC reaction (blue) with NADH standard (green).

UDP-sugar with a carboxylic acid functional group appears to be problematic on the NH_2 column. The UDP-GlcA standard was utilized in place of a UDP-HexNAcA standard because UDP-GlcA is commercially available and structurally similar. While UDP-ManNAcA is available commercially it is cost prohibitive as well as having a six-week turnaround time on production. Longer retention times on the NH_2 column results in peak broadening and loss of resolution. Detection of UDP-GlcA appears to be impossible due to its highly polar nature resulting in it sticking on the column and eluting so late that no peak was observed at the tested buffer conditions.

Previous literature supports the UDP-GlcA separation and detection on a HILIC-Z column, [21] so method development to detect UDP-HexNAcA sugars begun. It was

hypothesized that using ammonium acetate in basic conditions (pH 9.0) would give good results for separation and detection, as Agilent has used the same conditions for separation of similar highly polar organic metabolites such as nucleotides (ADP,ATP,GTP) and sugar phosphates (glucose-1-phosphate) in mammalian cell

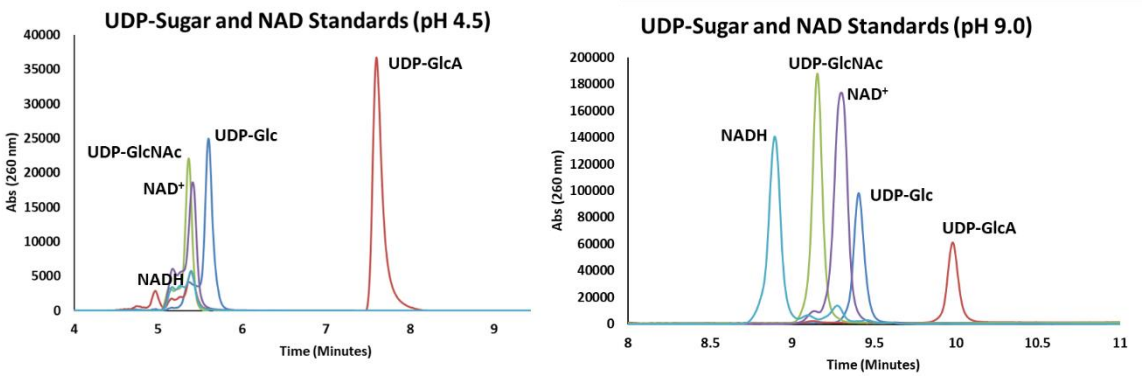

Figure 18. Comparison of separation of standards at pH 4.5 (Left) and pH 9.0 utilizing a 95%-50% A scouting gradient (Right). Chromatographic separation of UDP-Sugar standards on HILIC-Z column illustrating clean separations and good peak shape between UDP-Glc, GlcNAc, GlcA, NADH and NAD^+ at pH 9.0.

cultures.[23] Upon testing a range of pH's for the ammonium acetate buffer it was confirmed that basic conditions of pH 9.0 resulted in good separation of UDP-sugars (UDP-Glc, UDP-GlcNAc and UDP-GlcA) as well as NAD standards (NAD+ and NADH) (Fig. 18). Utilizing a more acidic pH of 4.5 similarly to the NH_2 column resulted in poor separation of NAD^+ and NADH as well as poor peak resolution. It was also found that in order to have good peak shape, that diluting samples in the mobile phase was necessary before injection. While this is good practice for general use in HPLC, it has never been an issue in the Troutman lab when using other columns such as reverse phase HPLC or the NH_2 column.

Once good standards separation was achieved, the MS was used for verification of standards by mass (Fig. 19 and 20). The masses found for UDP-Glc (565.04 m/z),

UDP-GlcNAc ([M-H]$^-$ 606.04 m/z), UDP-GlcA ([M-H]$^-$ 579.04 m/z), NADH ([M-H]$^-$ 664.12 m/z), and NAD$^+$ ([M-H]$^-$ 662.10 m/z and [M_1-H]$^-$ 540.06 m/z fragment corresponding to loss of nicotinamide) corresponded to what the exact calculated masses would be expected in negative ion ESI mode.

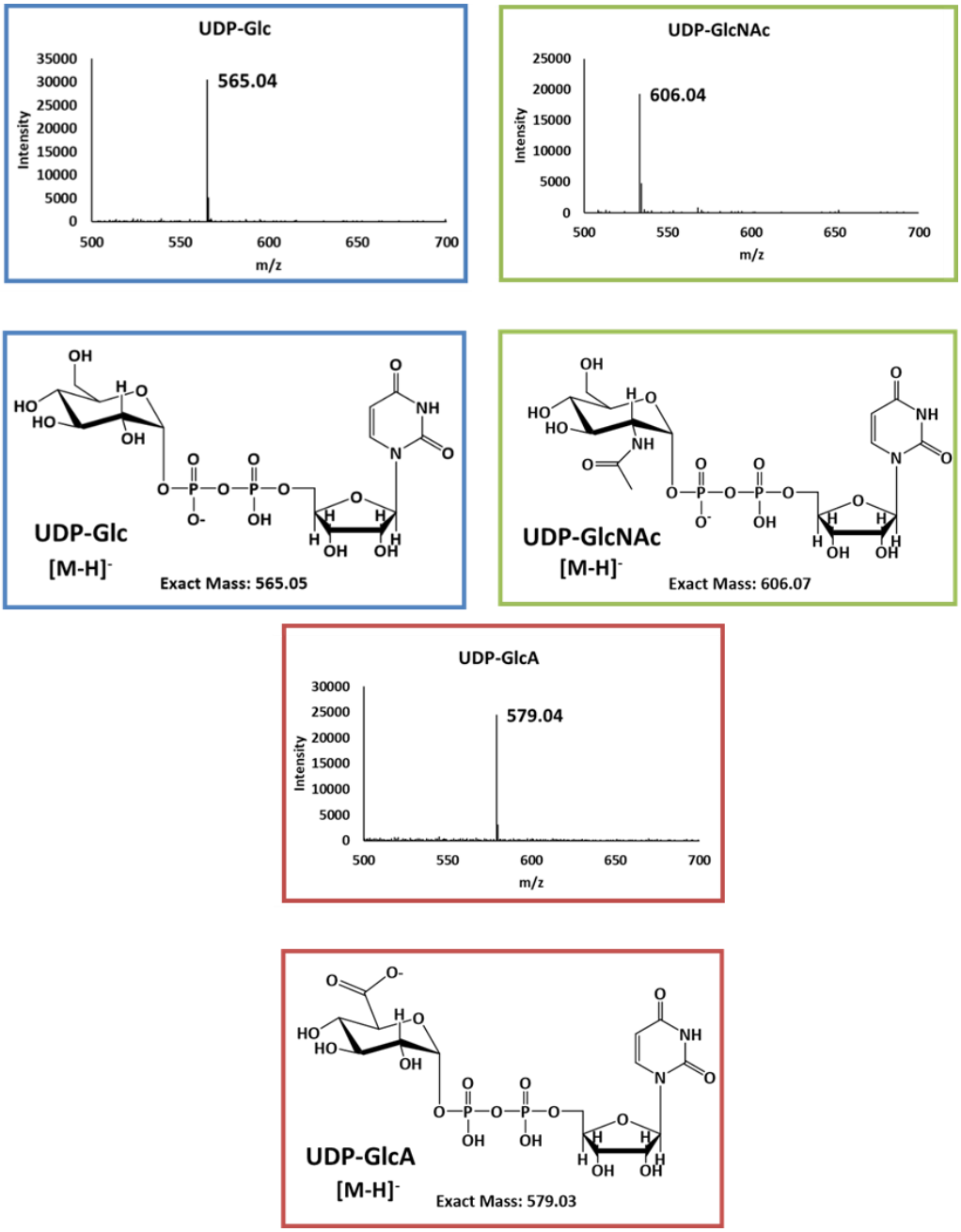

Figure 19. Detection of UDP-Sugar standards by LC-MS

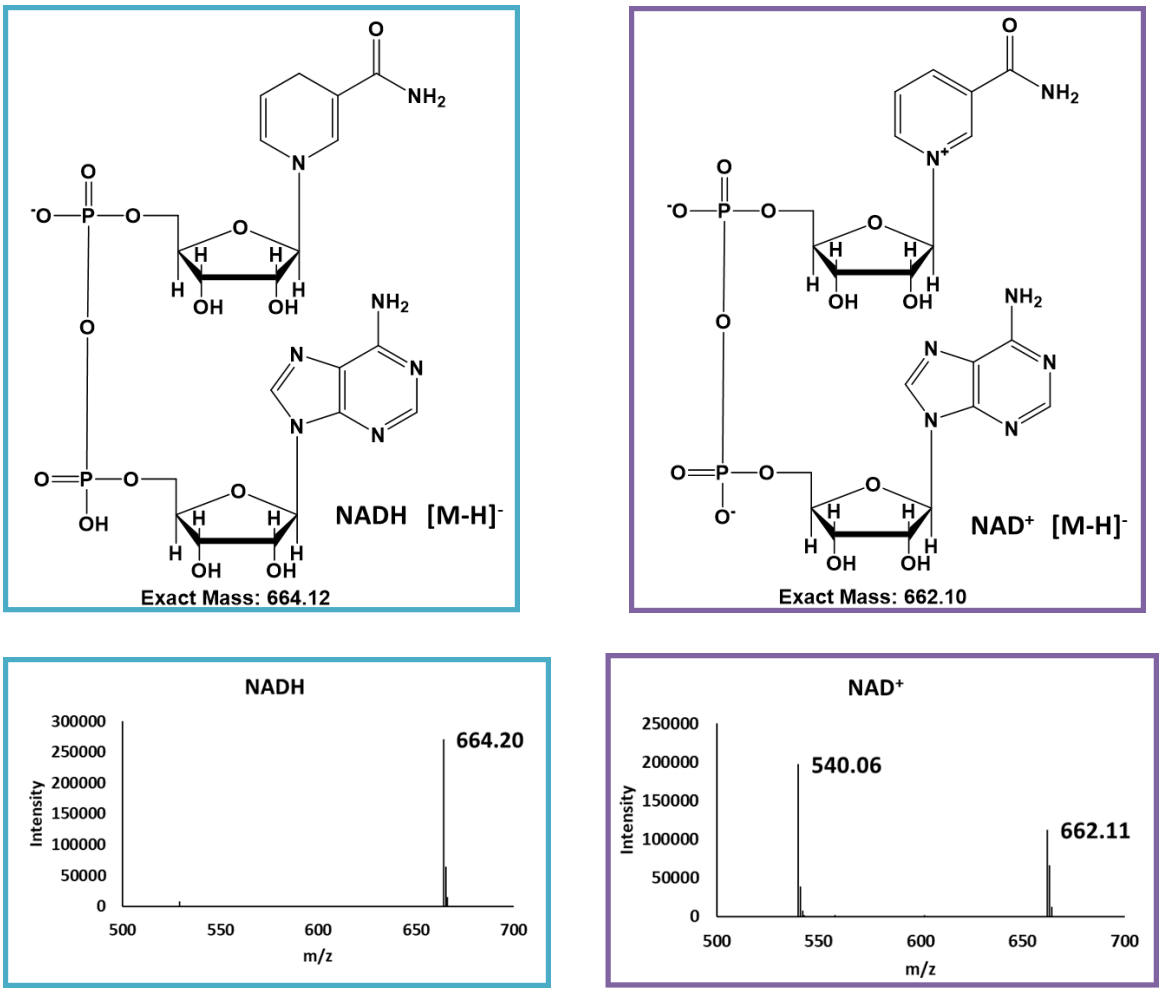

Figure 20. Detection of NADH and NAD^+ standards by LC-MS. Fragmentation of the nicotinamide results in the 540 m/z peak observed in NAD^+.

3.1.3 Analysis of UDP-HexNAcA enzymatic synthesis

After detection of standards on LC-MS, both a WecC and a coupled WecB-WecC reaction were injected on the HILIC-Z column. A peak corresponding to a UDP-HexNAcA sugar was separated chromatographically and identified by LC-MS in both reactions (Fig. 21). A sugar with a mass $[M-H]^-$ 620.05 m/z was found which could correspond to both UDP-GlcNAcA and UDP-ManNAcA making it unclear which

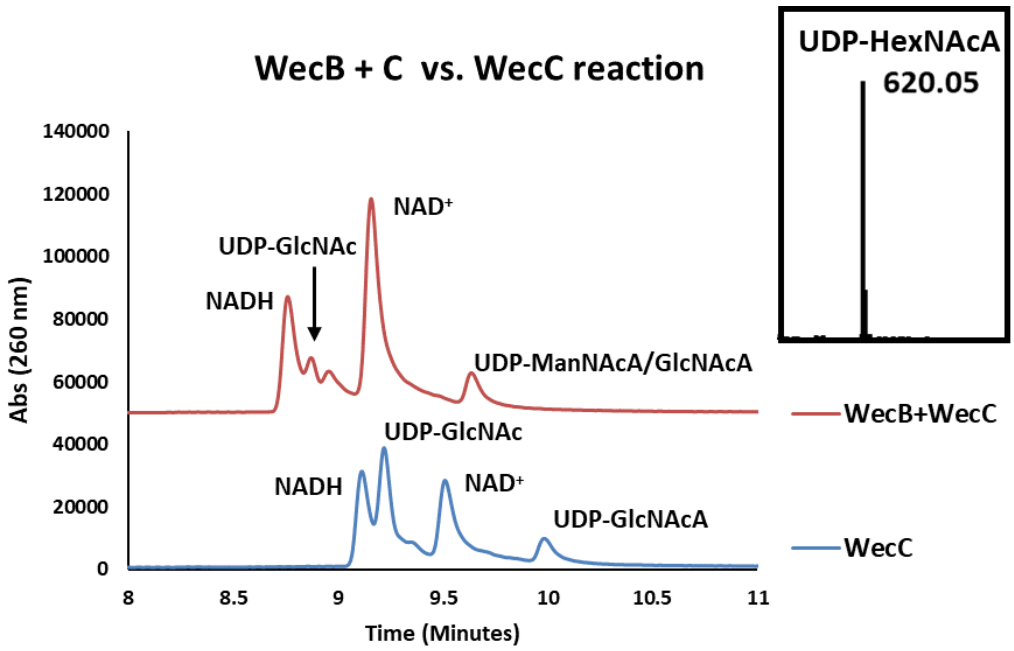

Figure 21. Comparison of Coupled WecB + WecC (red) reaction to WecC (blue) with peaks verified by mass on LC-MS. Both show the formation of a new peak to the right of NAD^+ with mass that confirms formation of a UDP-HexNAcA sugar in both reactions (inset). It is possible that there is a mixture of product being formed in the coupled WecB-WecC reaction.

product is being formed in the coupled WecB-WecC reaction. This suggests that WecC could accept UDP-GlcNAc as a substrate to form UDP-GlcNAcA. This finding has not been confirmed in the literature, and it appears that only Karawmura et al., had initially tested this but with 0.1 mM UDP-GlcNAc which is a vastly smaller amount of substrate (1975).[14]

The finding that WecC could produce UDP-GlcNAcA alone without the use of WecB questioned whether the WecB enzyme was working. Shallowing the gradient for the LC-MS method allowed earlier elution of products and detection of UDP-ManNAc in the WecB reaction (Fig. 22). Through integration of the peak areas for the WecB reaction it was found that there was 9% turnover to UDP-ManNAc consistent with the findings in previous literature.[12]

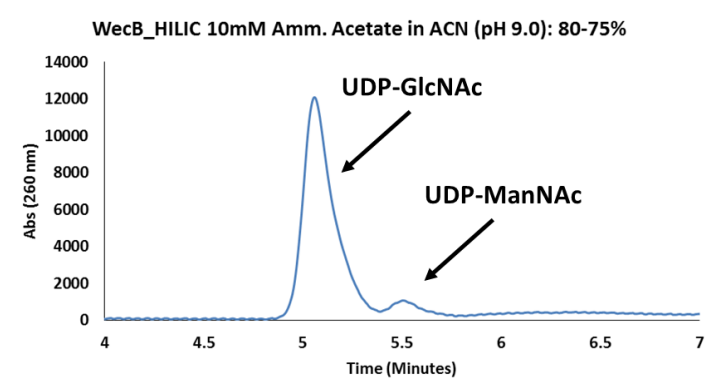

Figure 22. Detection of WecB reaction on HILIC-Z column. A shallower gradient of 80-75% 10 mM Ammonium Acetate in ACN achieved the necessary separation to observe formation of UDP-ManNAc

After confirmation of enzyme activity, the effect of changing conditions (pH, [NAD+], and [UDP-GlcNAc]) of the coupled WecB-WecC reaction and the formation of UDP-HexNAcA was observed. Of the pHs tested for the Tris-HCl buffer

[NAD⁺] (mM)	Average % UDP-HexNAcA
0.16	33±8
0.5	37±10
1	40±6
2	50±6
4.5	50±10
9	40±7

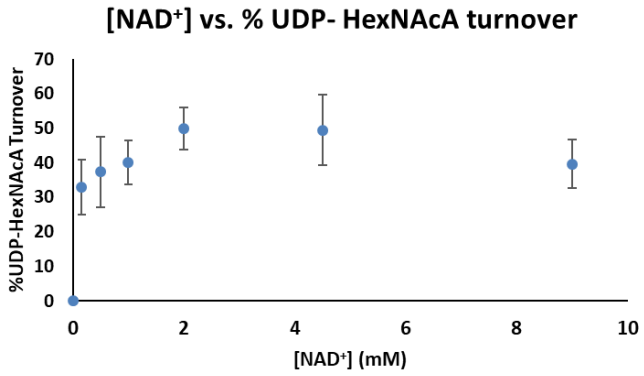

Figure 23. Scatter plot of [NAD+] vs. %UDP-ManNAcA turnover with accompanying table showing average numerical values and standard deviation (n=4).

(8.0, 8.6, and 9.0), the most UDP-HexNAcA was formed at pH 9.0 confirming literature results that a basic pH is needed for this reaction to be successful as the dehydrogenase, WecC, is most active at this pH.[15]

The effect of changing the [NAD+] was observed as well in relation to % of UDP-HexNAcA formed by integrating peak areas of the product and UDP-GlcNAc substrate. A scatter plot was produced and the average and standard deviation were calculated for the runs of varying concentrations (Fig. 23). It appears that changing the concentration of NAD^+ had little effect on turnover. The role of the concentration of

[UDP-GlcNAc] (mM)	Average % UDP-HexNAcA
0.25	47±9
0.5	49±12
0.75	34±13
1	50±10

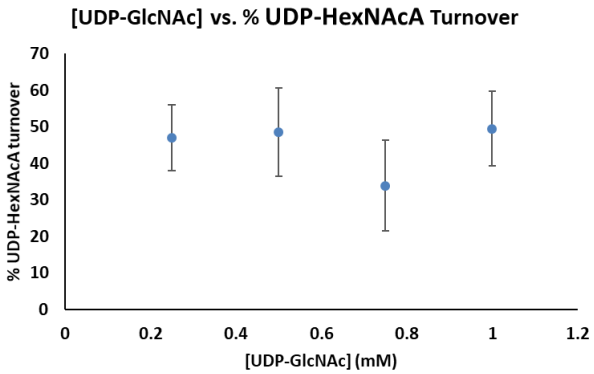

Figure 24. Scatter plot of [UDP-GlcNAc] vs. %UDP-ManNAcA turnover with accompanying table showing average and standard deviation (n=4). There were no significant differences observed when changing concentration of UDP-GlcNAc.

UDP-GlcNAc was investigated and the results are shown below in a table and scatter plot (Fig. 24). Results show that the effect of changing the concentration of UDP-GlcNAc had a minimal effect on the percentage of UDP-HexNAcA turnover.

Due to the novel finding of WecC utilizing UDP-GlcNAc, other sugars were tested including UDP-Glc, UDP-Gal, and UDP-GalNAc to see if WecC would turn any of them into UDP-sugar acids. Conversion of NAD^+ to NADH was observed but no new product was observed to be formed in any of these reactions. $NADP^+$ was also tested in

place of NAD^+ and production of UDP-GlcNAcA was observed, an activity that hasn't been confirmed in literature (Fig. 25). The surprising finding of UDP-GlcNAc acting as a substrate for WecC has made the acquisition of pure UDP-ManNAcA more difficult and made the formation of a mixture of UDP-ManNAcA and GlcNAcA in a coupled WecB-WecC reaction a possibility. A WecC reaction with pure UDP-ManNAc was set up to unequivocally make UDP-ManNAcA for testing with WecG, and part of this reaction mixture was mixed with a WecC reaction with UDP-GlcNAc and injected on the LC-MS to see if separation was possible between UDP-GlcNAcA and UDP-ManNAcA which was not observed (Fig. 26). So far separation has not been achieved between these two sugars on the HILIC column and could be impossible due to their highly polar nature which results in the much later elution times. It is also possible that a separation between

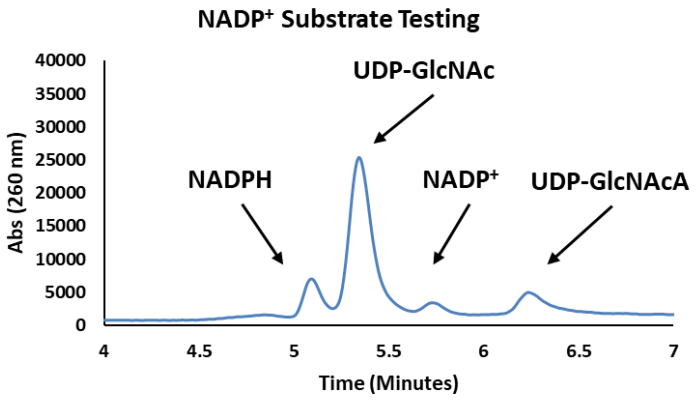

Figure 25. Reaction showing WecC utilizing $NADP^+$ in place of NAD^+ with formation of NADPH and producing UDP-GlcNAcA

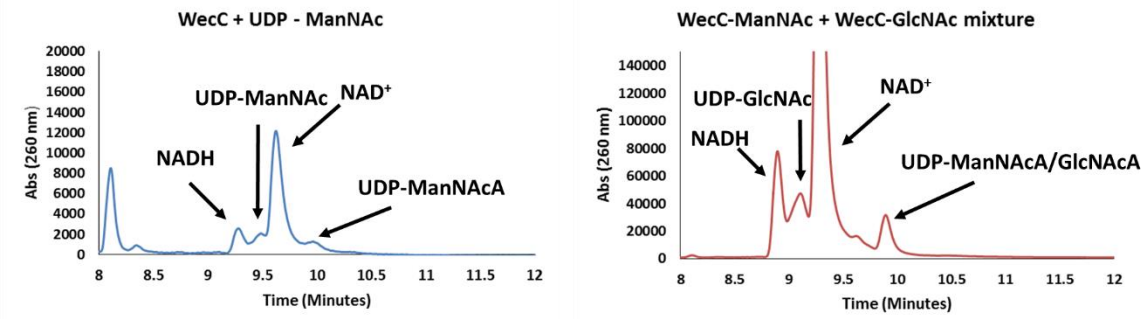

Figure 26. WecC and UDP-ManNAc reaction (blue) and mixture of WecC reactions with UDP-ManNAc and UDP-GlcNAc as starting substrates (red). Formation of UDP-ManNAcA was observed but when mixed with the other reaction there was no separation of UDP-ManNAcA and GlcNAcA

the two sugars was not observed because there was a larger concentration of the WecC UDP-GlcNAc reaction injected which could cause the UDP-GlcNAcA to bleed over into the UDP-ManNAcA peak. This experiment could be repeated, however the initial amount of pure UDP-ManNAc was limited to make UDP-ManNAcA without WecB and currently there is a barrier to getting more UDP-ManNAc. UDP-ManNAc could be isolated from an enzymatic WecB reaction however there is poor separation between UDP-GlcNAc and ManNAc which could result in an impure product, and the poor turnover to UDP-ManNAc could result in a waste of material. Chemo-enzymatic and chemical synthesis approaches have been used in the literature due to the difficult nature in acquiring UDP-ManNAc enzymatically but these approaches are technically difficult.[24, 25]

It was hypothesized that there may be a concentration of UDP-GlcNAc substrate or timepoint in the reaction that could significantly lower activity with WecC alone than in a coupled reaction. This is important because if there is a point where a minimal amount of UDP-GlcNAcA was produced by WecC reaction, the coupled reaction could be quenched and then isolated in order to guarantee only UDP-ManNAcA was formed. A concentration of UDP-GlcNAc at the literature K_M of 0.4 mM was used[14] as a starting point and smaller concentrations of 0.2, 0.1, and 0 mM were also used (Fig. 27). It was observed that there was no significant difference between the % turnover between the coupled and uncoupled WecC reactions. It was shown in this experiment, however, that WecC was able to form UDP-GlcNAcA at 0.1mM which Kawamura et al. had not observed (1975).[14] While the WecC reactions have activity at these lower concentrations of sugar substrate, the activity could be so poor at this level that it may not even be

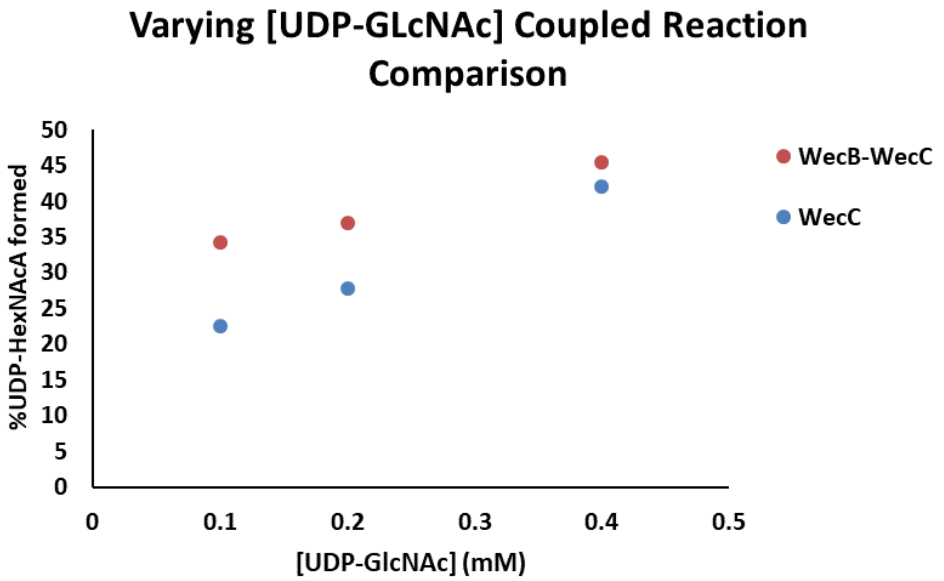

Figure 27. Varying [UDP-GlcNAc] and comparing a WecC only (blue) and coupled WecB-WecC reaction (red). Average values are plotted with n=4, and there appeared to be no significant difference between the coupled and uncoupled reaction.

possible to observe any meaningful differences. This brings into question as to whether the kinetics of WecC and UDP-ManNAc need to be reevaluated if there are not significant differences between the two reactions, however more runs could be done to improve consistency of the data set. Coupled and uncoupled WecC reactions were also set up and the time points of activity were monitored at 0.5,1, 2, and 3 hours (Fig. 28). Concentration of WecC was monitored at 3 µM and 1.5 µM. This experiment also did not result in any significant differences between the reactions, with still a significant amount of UDP-GlcNAcA formed with WecC only reactions. Variations in the reactions could be due to pipetting and the reaction mixture not being properly mixed when aliquoting. Decreasing the concentration of WecC in half also did not appear to affect the reaction.

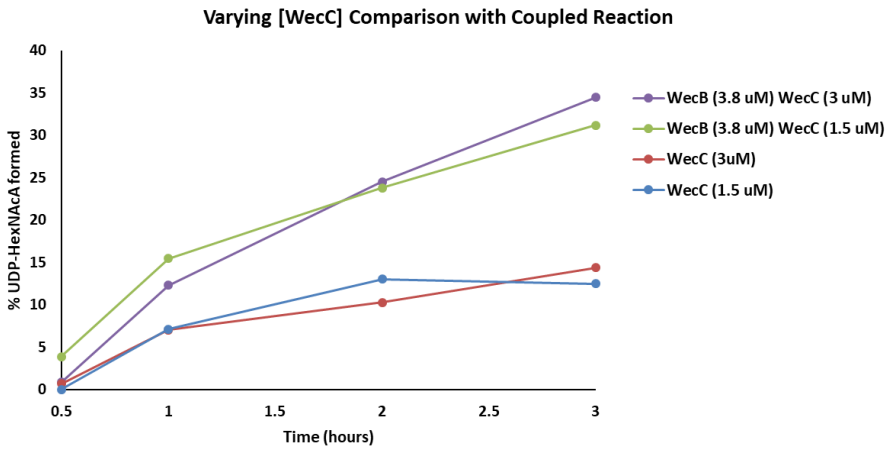

Figure 28. Varying [WecC] and comparing with coupled reaction over time points (0.5, 1, 2, and 3 hours) with averaged percent turnover plotted (n=3). No significant difference was observed between coupled and uncoupled WecC reactions. Decreasing the concentration of WecC did not have a significant effect on the formation of product.

The concentration of WecB was also tested by increasing to a very high amount of 20 uM while also testing the concentration of WecC at 3, 1, 0.5, and 0.75 µM. It was thought that if WecB was very concentrated that it would be favored as the acceptor for UDP-GlcNAc at a point where the concentration of WecC is low enough to not see any activity with just a WecC reaction. However, there was no discernable difference in turnover when changing concentration of WecC.

Since WecC demonstrated the conversion of UDP-GlcNAc to UDP-GlcNAcA which has not been documented in the literature, the kinetics of the WecC only reaction were tracked by taking time points and varying the UDP-GlcNAc concentration. This was made possible by tracking the formation of NADH through fluorescence and the development of a fluorescence experiment was designed based on literature precedent.[26] This assay works as NADH can emit fluorescence at 460 nm when excited by a 340 nm wavelength, whereas the oxidized NAD^+ form does not emit. When running the time point experiments a formation of NADH was observed in the presence of no substrate, which has been confirmed through HPLC runs as well. It was theorized that while WecC

will convert NAD^+ into NADH, that in the presence of an accepted nucleotide sugar substrate that the mechanism with sugar will take priority, which is why the run was not taken into account as background during the fluorescence assay. An example of the data produced by the plate reader assay is shown in Fig. 29.

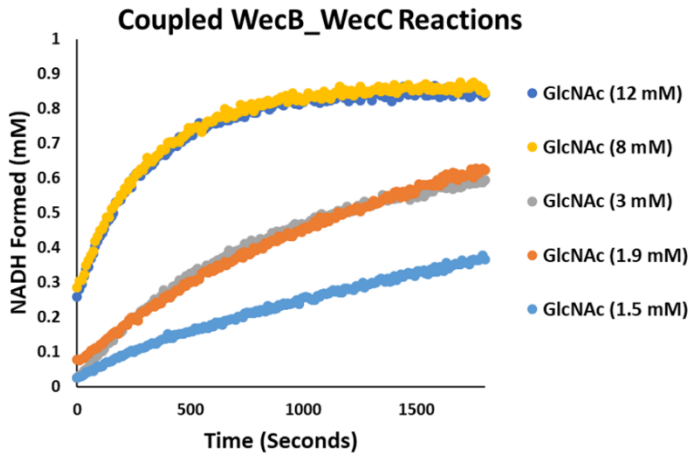

Figure 29. Fluorescence plate reader assay example for a range of concentrations of UDP-GlcNAc with 0.8 mM NAD^+. Relative fluorescence units (RFU) were converted to NADH formed (mM) through a standard curve.

The WecC reaction was compared to the coupled WecB-WecC reactions through a Michaelis-Menten plot (Fig. 30). From the Michaelis-Menten plot it is clear that the

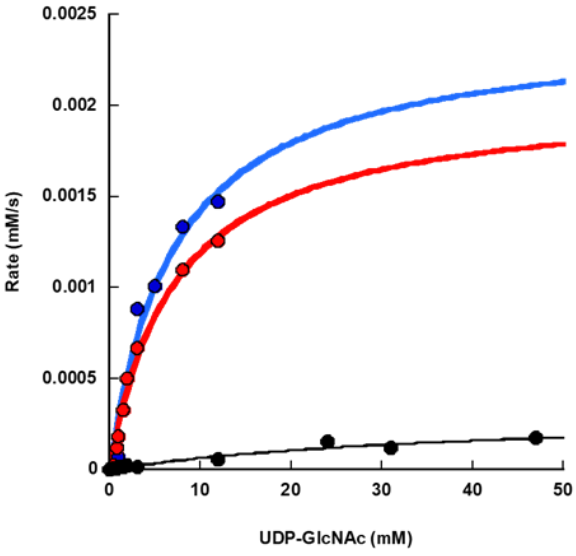

2 mM NAD+		
	Value	Error
Vmax	0.0024317	0.00064621
Km	7.0933	3.8116
Chisq	9.5661e-8	NA
R^2	0.95032	NA

NAD+ 1 mM		
	Value	Error
Vmax	0.0020412	0.00024279
Km	7.1151	1.6401
Chisq	2.8402e-8	NA
R^2	0.98046	NA

WecC only		
	Value	Error
Vmax	0.00032664	0.0001087
Km	43.214	24.874
Chisq	1.9829e-9	NA
R^2	0.94975	NA

Figure 30. Michaelis-Menten plots of WecC reaction (Black), coupled WecB-WecC reaction at 0.8 mM NAD^+ (Red), and coupled WecB-WecC at 2 mM NAD^+ (Blue) (runs were averaged with n=2). The WecC reaction is much slower than the coupled reactions.

WecC reaction happens at a much slower rate than both WecB-WecC reactions which reached saturation at approximately 8 and 12 mM of UDP-GlcNAc. Due to the much slower rate of reaction, much higher concentrations of UDP-GlcNAc needed to be used for the WecC reaction and saturation was still not observed. When increasing NAD^+ to 2 mM, the WecB-WecC reaction follows a similar plot than the one at 0.8 mM In order to do a quantitative comparison of these reactions, a Hanes Woolf plot was performed to do a linear fit of the data with the V_{max}, K_M, k_{cat}, catalytic efficiency (k_{cat}/K_M), and relative k_{cat}/K_M calculated (Fig .31). The V_{max}, K_M, k_{cat}, and k_{cat}/K_M were all significantly lower for WecC suggesting that while WecC can utilize UDP-GlcNAc as a substrate, that UDP-GlcNAc is kinetically unfavored due to weak binding (high K_M value) and poor turnover (low k_{cat} value) resulting in much lower catalytic efficiency . When increasing the concentration of NAD^+ to 2 mM the K_M of UDP-GlcNAc drops from 6.16 to 4.17 mM with a slightly lower catalytic efficiency, but this difference appears negligible in light of the error associated with the Hanes-Woolf Plots. The data suggests that UDP-ManNAc is the preferred substrate due to WecB making UDP-ManNAc that is being utilized by WecC in the coupled reaction. A kinetic point was found and confirmed by HPLC at 2mM NAD^+ where only the coupled WecB-WecC reaction produced UDP-HexNAcA product (Fig. 32). Only two runs of each data point were recorded and averaged due to limited UDP-GlcNAc, so more runs in the future could be attempted to improve the accuracy of the data set. In order to limit the number of assumptions made, it would be useful to test the kinetics of pure UDP-ManNAc and WecC and compare to the coupled WecB-WecC reaction to confirm similar behavior.

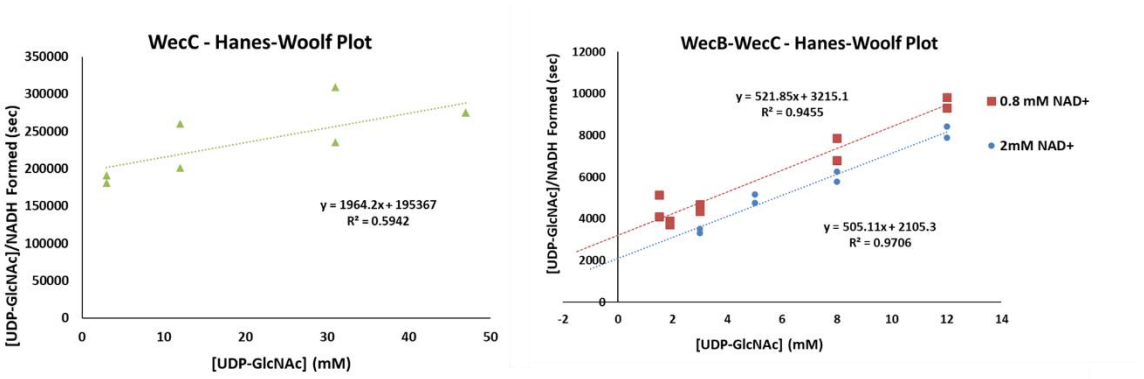

Reaction	Vmax (mM/sec)	K_M (mM)	k_{cat} (sec^{-1})	k_{cat}/K_M ($M^{-1}sec^{-1}$)	Relative k_{cat}/K_M ($M^{-1}sec^{-1}$)
WecC (0.8mM NAD^+)	5.09E-04	99.46	0.68	7	0.01
WecB-WecC (0.8mM NAD^+)	1.91E-03	6.16	2.55	415	0.66
WecB-WecC (2mM NAD^+)	1.98E-03	4.17	2.64	633	1

Figure 31. Hanes-Woolf plots of WecC (Left) and coupled WecB-WecC reactions (Right) with calculated Vmax, K_M, k_{cat}, catalytic efficiency (k_{cat}/K_M), and relative catalytic efficiency (bottom table). Based on initial results, the coupled WecB-WecC reactions are kinetically favored with the increase of NAD^+ greatly improving the catalytic efficiency by large decrease in K_M suggesting a stronger binding.

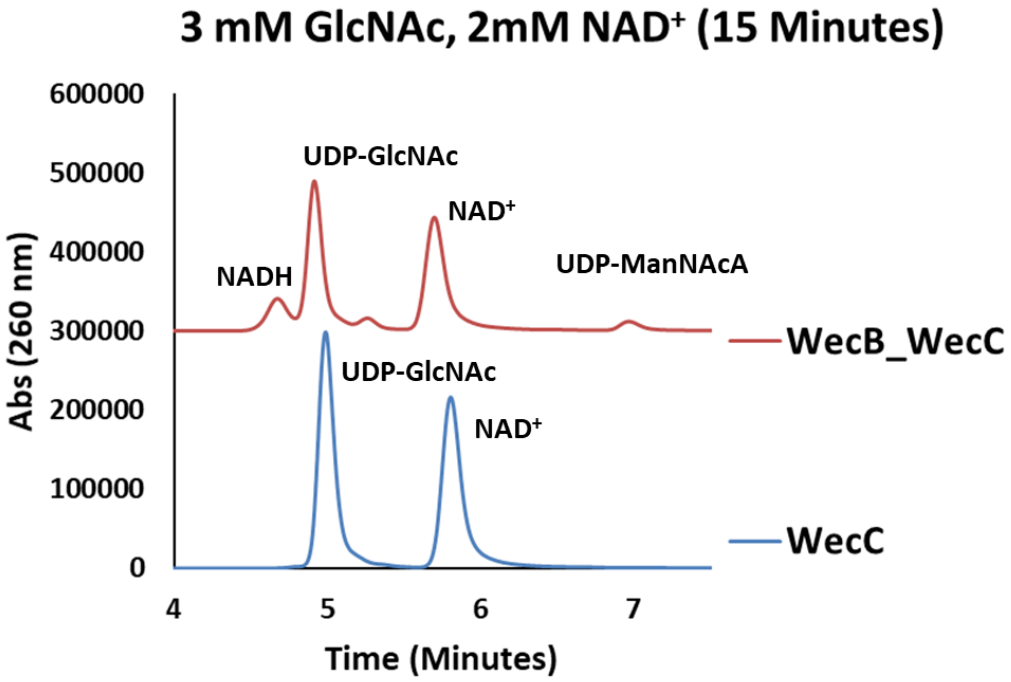

Figure 32. HPLC confirmation of 15-minute kinetic point of reactions with 3 mM UDP-GlcNAc and 2 mM NAD^+. No formation of NADH or UDP-HexNAcA product was observed in the WecC reaction (blue).

3.1.4 WecG Specificity Testing

While literature has identified WecG as a UDP-ManNAcA transferase, [15] purified WecG has not been tested *in vitro*, so both its activity and specificity was probed. Preliminary testing of WecG with WecB and WecC in *in vitro* one pot reactions suggested that the WecG transferase works with more than one substrate (Fig. 33).

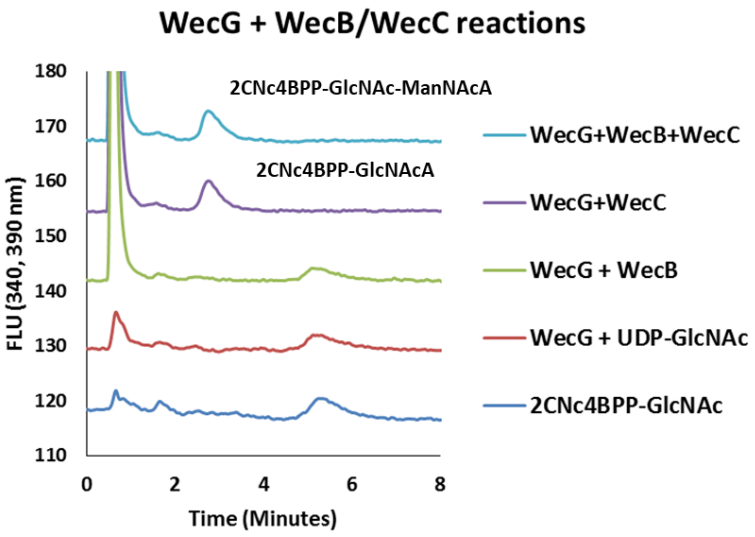

Figure 33. Results of testing WecG with WecB and WecC enzymes. A control 2CNc4BPP-GlcNAc (blue) shows a peak at a retention time of 4 minutes. Activity of turnover was witnessed with WecG, WecB, WecC, and UDP-GlcNAc (teal), WecG, WecC, and UDP-GlcNAc (purple) suggesting transfer of both UDP-ManNAcA and UDP-GlcNAcA

There was complete turnover of the 2CNc4BPP-GlcNAc peak at 6 minutes with the reaction that includes WecG, WecB, WecC, and UDP-GlcNAc suggesting successful transfer of presumed UDP-ManNAcA after being converted. However turnover was also observed for WecG with WecC showing transfer of presumed UDP-GlcNAcA. No turnover was observed with the WecB reaction or with just UDP-GlcNAc.

In order to confirm the activity of WecG found in the literature, 5 µL aliquots of WecC and UDP-ManNAc reaction were used for UDP-ManNAcA. This transfer activity

was compared to UDP-GlcNAcA, with both sugars being tested with 2CNc4BPP-Glc and 2CNc4BPP-Gal. (Fig. 34) Turnover was observed for both UDP-ManNAcA and UDP-GlcNAcA with 2CNc4BPP-GlcNAc. Complete turnover of 2CNc4BPP-Glc was observed as well with UDP-GlcNAcA and partial activity with UDP-ManNAcA. The partial activity of transfer with UDP-ManNAcA could be attributed to the fact that an

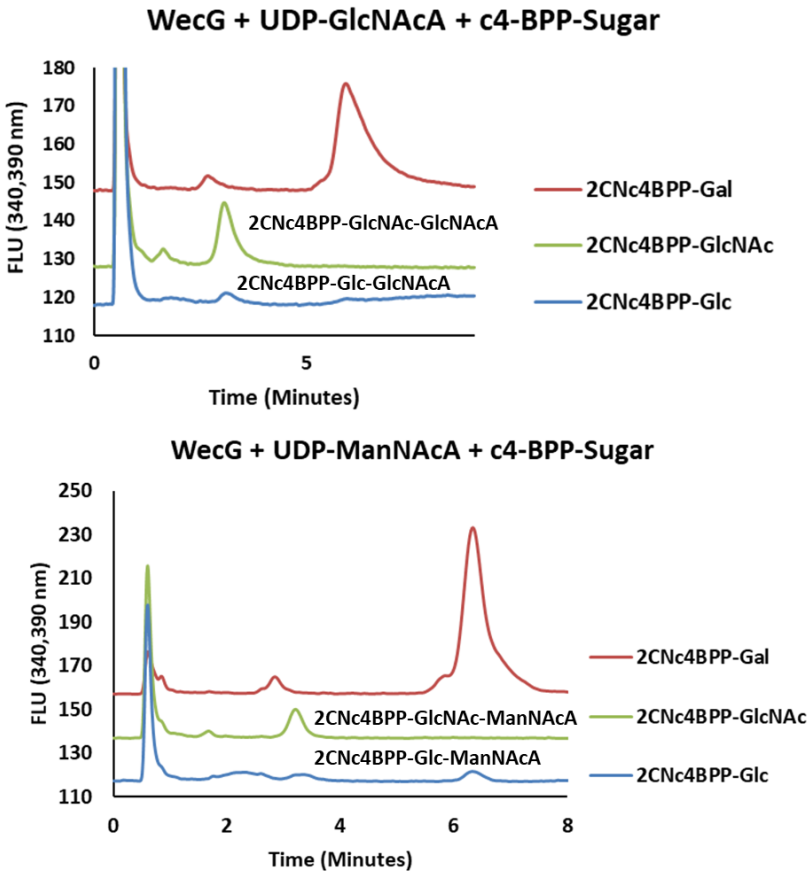

Figure 34. Testing of 2CNc4BPP substrates with UDP-GlcNAcA (Top) and UDP-ManNAcA (Bottom) with WecG. WecG shows activity with both 2CNc4BPP-GlcNAc and 2CNc4BPP-Glc.

aliquot of the same reaction was used as for testing 2CNc4BPP-GlcNAc. It could be that 2CNc4BPP-Glc requires a higher concentration of UDP-ManNAcA in order for WecG to transfer to 2CNc4BPP-Glc. This experiment needs additional follow up.

A range of nucleotide sugars that are commercially available were tested as well with WecG and 2CNc4BPP-GlcNAc (Fig. 35). Of the five sugars tested, none demonstrated turnover or activity with the c4 isoprenoid probe with evidence showing that WecG will only accept UDP-ManNAcA or GlcNAcA as a substrate.

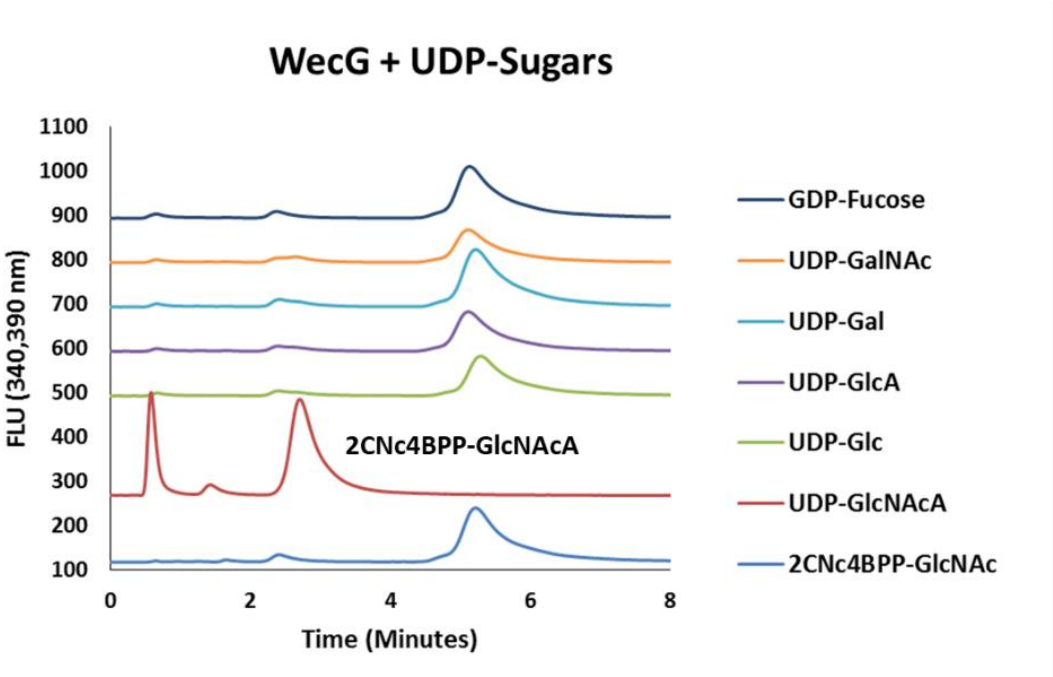

Figure 35. Testing of WecG with common nucleotide sugars with positive control (red) confirming WecG activity with UDP-GlcNAcA. WecG shows no signs of transferring any other sugars besides UDP-GlcNAcA and UDP-ManNAcA.

3.2 *H. pylori* glycosyltransferases

3.2.1 Cloning results

In order to begin studying the *H. pylori* glycosyltransferases, seven of the glycosyltransferases needed to be cloned in order to start expressing the proteins to study activity. LIC cloning of Hp_G27_190, 579, 607, 645, 952, 1236, and 1518 was found to be successful and efficient. For the PCR isolation of the genes (sizes listed in Table 2) a 50°C annealing temp was found to be successful for annealing the gene into the plasmid except for Hp_G27_607 which had a nonspecific band (Fig. 36).

Table 2. The seven Hp_G27 genes and their length (in bp) that needed to be cloned. To increase throughput, LIC was utilized

Gene	Gene length (bp)
Hp_G27_190	1020
Hp_G27_579	558
Hp_G27_607	1680
Hp_G27_645	810
Hp_G27_952	1167
Hp_G27_1236	1038
Hp_G27_1518	999

For Hp_G27_607 a temperature gradient was performed (temperatures 51.1, 53, 54.7, and 57.8°C were tested) and an optimal annealing temperature was found to be 58°C which resulted in a single band as seen in Figure 36 (B). All completed plasmids were transformed successfully into DH5-α cell lines and verified by Sanger sequencing.

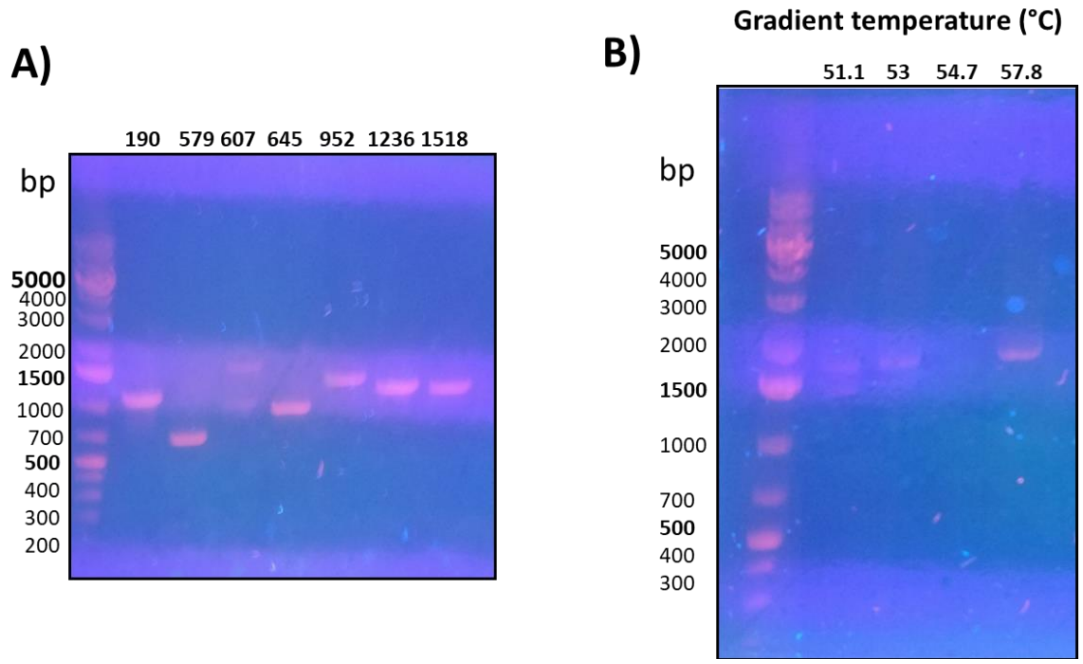

Figure 36. (A) PCR results of using an annealing temp of 50°C with Hp_G27_607 showing a nonspecific band at around 1000 bp. (B) temperature gradient results for Hp_G27_607. 57.8°C shows a single band with nonspecific bands at 51.1 and 53°C. No bands were found when using an annealing temp of 54.7°C

3.2.2 Preliminary protein expression and analysis

After successful construction of plasmids of *H. pylori* glycosyltransferase genes, the process was begun for expressing the proteins of interest. Hp_G27_190 and 1518 were chosen to be the first genes of interest to be expressed and transformed into a C41 expression strain. Both 1518 and 190 were expressed successfully (Fig. 37) with their concentrations and sizes listed in Table 3. Analysis of transmembrane protein domains in TMHMM, [27] a method for predicting protein topology, suggests 1518 is an initiating transferase with 11 transmembrane domains similar to WecA in the ECA

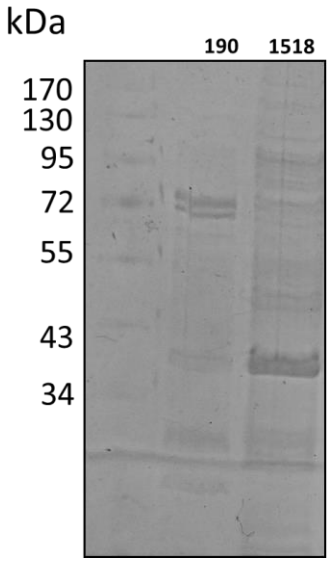

Figure 37. SDS-PAGE of Hp_G27_190 (40 kDa) and 1518 (38 kDa)

pathway, a known initiating phosphoglycosyltransferase (Fig. 38). The protein sequence of 1518 has also been analyzed through NIH pBlast with matches with the MraY-like family, a phosphoglycosyltransferase responsible for the initiating transfer step of peptidoglycan production in bacteria which has a characteristic 10 trans-membrane domains. When utilizing the protein alignment software, EMBOSS Needle, it was found that 1518 only has a 19.8% match in identity and a 33.0% similarity to MraY found in *E. coli* (Fig. 38).

Table 3. Sizes and concentration of Hp_G27_1518 (a membrane protein and identified phosphoglycosyltransferase) and 190 (a glycosyltransferase)

Protein	Type of protein	Molecular Weight (kDa)	Concentration (mg/ml)
Hp_G27_1518	Membrane	38	0.45
Hp_G27_190 (RfaJ-2)	Soluble	40	0.45

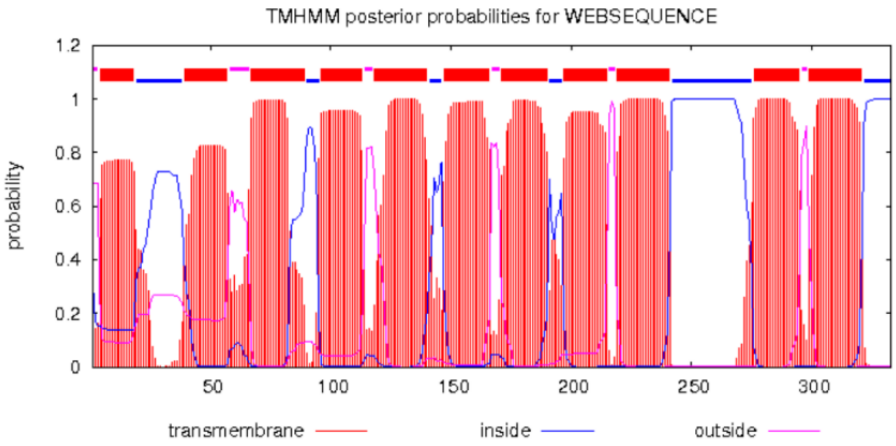

Figure 38. TMHMM analysis of Hp_G27_1518 predicting that 11 transmembrane domains exist in this protein similar to the initiating phosphoglycosyltransferase WecA

```
# Length: 424
# Identity:      84/424 (19.8%)
# Similarity:   140/424 (33.0%)
# Gaps:         155/424 (36.6%)
# Score: 165.0
#
#
#=======================================

HpG27_1518         1 --------------------------MLYFLTSLFICSLIVLWSKKSML-     23
                                                ::..||:|||.    ||....|:
MRAY_ECOLI         1 MLVWLAEHLVKYYSGFNVFSYLTFRAIVSLLTALFIS----LWMGPRMIA     46

HpG27_1518        24 ---------FVDNANKIQGFHHARTPRAGGLGIFLSFVLAYLFEPFEA-P     63
                             .|.|......|....||..||:.|..:.|::.|...:.: |
MRAY_ECOLI        47 HLQKLSFGQVVRNDGPESHFSKRGTPTMGGIMILTAIVISVLLWAYPSNP     96

HpG27_1518        64 FKG--FFVFLGLSLVFLSGFLEDINLSLSPKIRLILQ----------AVG    101
                     :..  ..|.:|..::   ||::|....:....:.::.          |:|
MRAY_ECOLI        97 YVWCVLVVLVGYGVI---GFVDDYRKVVRKDTKGLIARWKYFWMSVIALG    143

HpG27_1518       102 VICII-------SSTPLVV---SDFSPLFSLPYFIAFLFAIFMLVGISNA    141
                     |...:       .:|.|||   .|..|...|.|   .|.|.|::||..||
MRAY_ECOLI       144 VAFALYLAGKDTPATQLVVPFFKDVMPQLGLFY---ILLAYFVIVGTGNA    190

HpG27_1518       142 INIIDGFNGL--------ASGICAI----------TLLVIHYIDPSSLSC    173
                     :|:.||.:||        |.|...:          :.|.|.|:..:....
MRAY_ECOLI       191 VNLTDGLDGLAIMPTVFVAGGFALVAWATGNMNFASYLHIPYLRHAGELV    240

HpG27_1518       174 LLAYMV----LGFMVLNFPLGKIFLGDGGAYFLGLVCGISLLHLSLEQKI    219
                     ::...:    |||:..|....::|:||.|:..||...||..:.|..|..:
MRAY_ECOLI       241 IVCTAIVGAGLGFLWFNTYPAQVFMGDVGSLALGGALGIIAVLLRQEFLL    290

HpG27_1518       220 SVFFGLNLMLYPVVEVLFSILR---RKIKRQKATMPDNLHLHTLLFQFLQ    266
                     .:..|:.     |||.|..||:   .|::.|:.....:|.|..|
MRAY_ECOLI       291 VIMGGVF-----VVETLSVILQVGSFKLRGQRIFRMAPIHHHYEL-----    330

HpG27_1518       267 QRSFNYPNP-------LCALILILCNLPFILISVFFRLNPYALIAISLVF    309
                        ..:|.|       :.:|:|:|..|..:.:.
MRAY_ECOLI       331 ---KGWPEPRVIVRFWIISLMLVLIGLATLKVR-----------------    360

HpG27_1518       310 IACYLIGYAYLNRQVYALEKRAFQ    333

MRAY_ECOLI       361 ------------------------    360
```

Figure 39. EMBOSS Needle protein alignment of Hp_G27_1518 with MraY in *E. coli* showing low matches in identity and similarity.

Hp_G27_190 was also picked as it was shown in preliminary cloning trials to amplify in *E. coli* as well as Hp_G27. Hp_G27_190 was predicted to be a soluble protein based on TMHMM analysis predicting no transmembrane domains (Fig. 40). Upon further investigation Hp_G27_190 was found to be also known as RfaJ-2, a

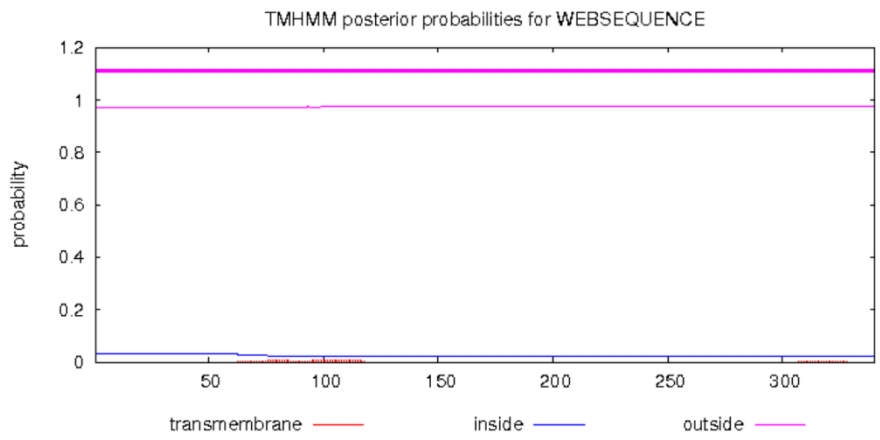

Figure 40. TMHMM analysis of Hp_G27_190 predicting that no transmembrane protein domains exist indicating that 190 is likely a soluble protein.

glycosyltransferase found in other Gram negative bacteria important in the biosynthesis of the lipopolysaccharide core through sequence analysis as well as gel analysis of lipopolysaccharides produced by *rfaJ* mutants of interest.[28] RfaJ-2 has been identified to add a glucose onto a galactose attached to the lipopolysaccharide in the outer core (Fig. 41). While this information could help elucidate the specificity of the RfaJ-2 found in *H. pylori*, comparing the protein sequence of Hp_G27_190 with RfaJ-2 in *E. coli* shows a 14.4% match in identity and 26.1% in similarity showing that there is still little known about the activity of Hp_G27_190 (Fig. 42).

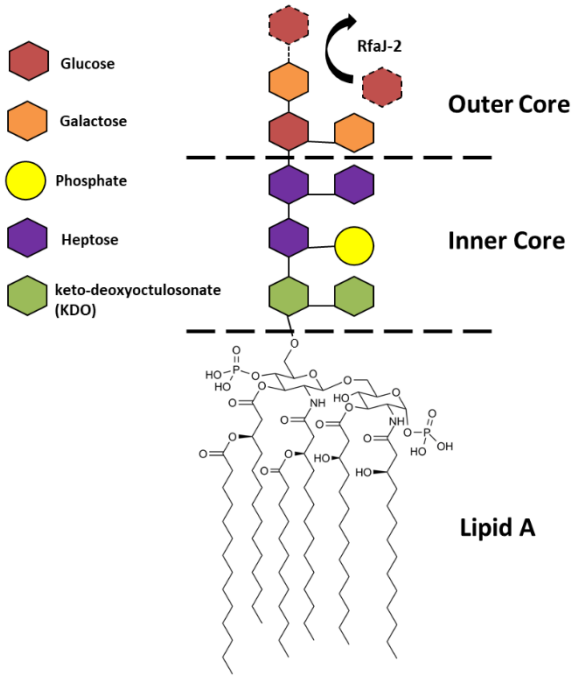

Figure 41. Schematic showing role of RfaJ-2 in lipopolysaccharide core biosynthesis. RfaJ-2 is a glycosyltransferase that transfers a glucose on a galactose in the outer core which is assembled on top of the inner core sugars anchored by lipid A.

```
# Length: 452
# Identity:      65/452 (14.4%)
# Similarity:   118/452 (26.1%)
# Gaps:         233/452 (51.5%)
# Score: 100.5
#
#
#=======================================

HP_G27_190         1 MVENLSAENVAKLEETIAPFSAFSSIEFLDITDKELEPRHNYYKLDALIA     50

RFAJ2ECOLI         1 --------------------------------------------------       0

HP_G27_190        51 SEIKKLYLKLNAFSQKRFSKM----------------IMCRFFFAS----     80
                        :|.|.::|||.:                |...|.:.:
RFAJ2ECOLI         1 ---------MNEFIKERFSYLADNKKENAPELNVSYGIDKNFLYGAGVSI     41

HP_G27_190        81 ---LFPQYDKMIMFDVDTLFVND---------------------ISESFF    106
                        |....|...:|.|.|.:|:|                     |...:|
RFAJ2ECOLI        42 SSVLINNSDINFVFHVFTDYVDDDYLKSFNETAKQFNTSIIVYLIDPKYF     91

HP_G27_190       107 IPLGTHYFGAVRE--------------KDLIAMD-----RNSAKDLYEL-    136
                     ..|.|..|.:...              ..|:.:|     :.|.|.|.|:
RFAJ2ECOLI        92 ADLPTSQFWSYATYFRVLSFEYLSESISTLLYLDADVVCKGSLKPLTEII    141

HP_G27_190       137 ---------------RQMRAKSIGVADAFPNLEEAQILFDNYFNAGFLAL    171
                                  ::..||.:.:.:          :...|||||.:.:
RFAJ2ECOLI       142 FKDEFAAVIPDNDSTQEACAKRLNIPE----------MNGRYFNAGVIYV    181

HP_G27_190       172 NLKLWREENLENQLIGFFLLKNE----KLLFPEQDALCF------VCRGR    211
                     |||.|.|.||...|:.  ||:.|    .|.:.:||||..      :..|:
RFAJ2ECOLI       182 NLKKWHEANLTPYLLK--LLRGETKYGSLKYLDQDALNIAFNMNNIYLGK    229

HP_G27_190       212 ILELPYSY------NAHPSFLDTPSFPSIKEACMLHFWG-DKPWKLLSVI    254
                     ..:..|:.      .:|..|..|.:..::    ::|:.| .|||...:..
RFAJ2ECOLI       230 DFDTIYTLKNELHDRSHRKFQQTITDKTV----LIHYTGITKPWHSWAGY    275

HP_G27_190       255 DAKEWHEVLIQT------PFKDAYFNAPFLDHLFESLQNMEKE-------    291
                     .:..:..:..:.      |.|:|           .::..|:|:
RFAJ2ECOLI       276 PSASYFNIAREQSPWKKYPLKEA-----------RTVAEMQKQYKHLFAH    314

HP_G27_190       292 ---IHALNKILSFSDKRHSFESLLPRLSSKLLIEFLLFKIKQKVKRLIKR    338
                        |..:..::.:..|:
RFAJ2ECOLI       315 GEYIKGITSLIKYKLKK---------------------------------    331

HP_G27_190       339 VF    340

RFAJ2ECOLI       332 --    331
```

Figure 42. EMBOSS Needle protein alignment of Hp_G27_190 with RfaJ-2 in *E. coli* showing low matches in identity and similarity.

CHAPTER 4: CONCLUSIONS AND FUTURE WORK

4.1 *in vitro* ECA analysis

The development of an LC-MS method to detect the UDP-HexNAcA product as well as formation of UDP-ManNAc with the HILIC-Z column has proven effective for detecting nucleotide sugars with a carboxylic acid functional group, which was not possible on an NH_2 column. The lower concentration of ammonium acetate buffer needed for separation allows using MS inline, however there appears to be difficulty in separation between UDP-ManNAcA and GlcNAcA.

With the surprising discovery that WecC can use UDP-GlcNAc as a substrate and also utilize $NADP^+$ in place of NAD^+, there appears to be more of a knowledge gap about the activity of the WecC dehydrogenase than previously thought. To this end, it is currently unclear whether only UDP-ManNAcA is being produced in a coupled WecB-WecC reaction and what percentage is being produced based on testing on the HPLC. Testing has been attempted to probe further into the dynamics of a coupled WecB-WecC reaction to see if there is a way to limit the WecC activity such that it only allows UDP-ManNAc to be utilized, however current research does not reveal any clear trends and more testing is required.

A kinetic assay with UDP-GlcNAc as a substrate for WecC currently shows that the K_m and k_{cat} found that the catalytic efficiency of WecC is very poor when interacting with UDP-GlcNAc which suggests that UDP-ManNAc is the preferred substrate for this enzyme as previously reported.[13] Also, testing the kinetics with a coupled reaction could mean that ,since WecB only results in a 10% yield of UDP-ManNAc, the actual K_M of the WecC reaction is actually 10-fold lower due to the limiting effect of the epimerase.

To confirm this, a kinetics assay would need to be performed with pure UDP-ManNAc and WecC. With this reasoning it could be argued that during the coupled reaction with WecB that only the production of UDP-ManNAcA would be favored. In order to confirm that there is only UDP-ManNAcA in an enzymatic reaction, this product would need to be analyzed with NMR to verify the stereochemistry.

At this time, the surest way to form UDP-ManNAcA is to use pure UDP-ManNAc alone with WecC. The epimerase WecB exhibits a poor product yield of 9% UDP-ManNAc formation which may be why recent experiments since Kawamura et al.'s initial experiments have gone the route of using synthetic approaches to produce UDP-ManNAc (1979).[13]

Dr. Xi Chen's lab of UC-Davis who sent a small amount of UDP-ManNAc for analytical testing has documented a chemo-enzymatic approach to making UDP-ManNAc that appears to be the least difficult approach, but still has caveats (2012).[24] A kinase such as NahK is used to transfer a phosphate group upon a sugar of interest, and then the UDP-Sugar pyrophosphorylase (BLUSP) from *B. longum* is used to add a uridine monophosphate to the phosphate sugar. Results show that starting with commercially available ManNAc is not possible because of the possible specificity of BLUSP. A successful route was found by starting with mannosazide ($ManN_3$) which is not commercially available and must be synthesized, and then catalytic hydrogenation to produce UDP-$ManNH_2$ is necessary followed by acetylation of the amino group to yield UDP-ManNAc, which adds to the complexity of this route. This approach could be considered if enzymatic synthesis of UDP-ManNAcA remains ambiguous.

WecG's *in vitro* activity has been successfully verified through the use of UDP-ManNAcA and showing production of the 2 sugar lipid intermediate, BPP-GlcNAc-ManNAcA. A future goal is to successfully produce the completed ECA, GlcNAc-ManNAcA-Fuc4NAc. In order to complete this TDP-Fuc4NAc needs to be synthesized as it is not commercially available. In the ECA pathway, TDP-Fuc4NAc is produced through the transfer of glucose-1-phosphate (P-Glc) onto a demoxythymidine triphosphate (dTTP) to yield thymidine diphosphate glucose (TDP-Glc). TDP-Glc is then converted to TDP-Fuc4NAc through the involvement of RmlB, WecE, and WecD.[29] Currently an undergraduate is working on this part of the Trouman lab in a collaboration, and the goal is to eventually complete the ECA and use a polymerase, Wzy, to elongate the oligosaccharide to be able to use for further experiments, including potentially design of glycogen based antigens.

So far data has shown that specificity for WecG is not limited to 2CNc4BPP-GlcNAc and UDP-ManNAcA. WecG also appears to work with UDP-GlcNAcA and 2CNc4BPP-Glc as a lipid anchor substrate. Since WecG can produce other products *in vitro* other than the lipid II intermediate, BPP-GlcNAc-ManNAcA, documented in the ECA pathway this brings into question if there are other sugar products that WecG may assemble inside of the cell. Also, since WecG transfers UDP-GlcNAcA, it could suggest that the ECA could be a mixture of GlcNAc-ManNAcA-Fuc4NAc and GlcNAc-GlcNAcA-Fuc4NAc and not just pure GlcNAc-ManNAcA-Fuc4NAc as the literature suggests. However, previous use of a precise analytical method such as NMR leaves little doubt in the structure of the second sugar in ECA that occurs naturally. [4] There could be

discrepancies in behavior between purified *in vitro* WecG and *in vivo* WecG that has yet to be studied.

The specificity of WecG is also being compared with a WecG homologue, BoWecG, found in *B.Ovis* in a collaboration with another graduate student and activity has already been shown with transfer of UDP-GlcNAcA. Goals of this collaboration include comparing WecG and BoWecG through UDP or 2CNc4BPP sugar substrate specificity.

4.2 *H. pylori* biosynthetic pathway

LIC was effectively used to successfully complete the cloning of the 13 glycosyltransferases identified by the Dube Lab in the *H. pylori* biosynthetic pathway. Currently, only Hp_G27_1518 and 190 (RfaJ-2) have been successfully expressed. Due to the large number of glycosyltransferases of interest to study *in vitro* work remains to completely study the glycosyltransferases in the *Helicobacter* pathway, and the goal of this research was to lay the ground work for the project by cloning and starting some of the protein expressions.

Currently the Troutman lab is continuing investigation into the *H. pylori* pathway by first probing the initiating transferase (1518) for activity by testing it with a fluorescent 2CNA-BPP probe and a library of nucleotide sugars to see which one it will transfer. Preliminary results suggest that this initiating transferase transfers a phosphate GlcNAc from UDP-GlcNAc showing WecA-like activity. However, this transfer could be due to WecA getting expressed by the gene so the purified plasmid of 1518 is being transformed into a Δ*wecA* bacterial strain. After the activity of 1518 is confirmed, determination of the next glycosyltransferase in the pathway will be the next step.

REFERENCES

1. National Research Council (US) Committee on Assessing the Importance and Impact of Glycomics and Glycosciences. (2012). Transforming Glycoscience: A Roadmap for the Future. The National Academies Collection: Reports funded by National Institutes of Health. Washington (DC): National Academies Press (US) National Academy of Sciences.
2. Whitfield, C. (2006). Biosynthesis and Assembly of Capsular Polysaccharides in Escherichia coli. *Annual Review of Biochemistry*, 75(1), 39-68.
3. Krasnova, L., & Wong, C. H. (2016). Understanding the Chemistry and Biology of Glycosylation with Glycan Synthesis. *Annu Rev Biochem*, 85, 599-630. doi:10.1146/annurev-biochem-060614-034420
4. Erbel, P. J. A., Barr, K., Gao, N., Gerwig, G. J., Rick, P. D., & Gardner, K. H. (2003). Identification and Biosynthesis of Cyclic Enterobacterial Common Antigen in Escherichia coli. *Journal of Bacteriology*, 185(6), 1995-2004. doi:10.1128/jb.185.6.1995-2004.2003
5. Basu, S., Kuhn, H.-M., Neszmelyi, A., Himmelspach, K., & Mayer, H. (1987). Chemical characterization of enterobacterial common antigen isolated from *Plesiomonas shigelloides* ATCC 14029. European Journal of Biochemistry, 162(1), 75-81. doi:doi:10.1111/j.1432-1033.1987.tb10544.x
6. Barr, K., Nunes-Edwards, P., & Rick, P. D. (1989). In vitro synthesis of a lipid-linked trisaccharide involved in synthesis of enterobacterial common antigen. *Journal of Bacteriology*, 171(3), 1326–1332.
7. Champasa, K., Longwell, S., Eldridge, A., Stemmler, E., & Dube, D. H. (2013). Targeted Identification of Glycosylated Proteins in the Gastric Pathogen *Helicobacter pylori* (Hp)*. *Molecular & Cellular Proteomics*, 12(9). doi:10.1074/mcp.M113.029561
8. Koenigs, M. B., Richardson, E. A., & Dube, D. H. (2009). Metabolic profiling of *Helicobacter pylori* glycosylation. *Mol Biosyst*, 5(9), 909-912. doi:10.1039/b902178g
9. Jorgenson, M. A., Kannan, S., Laubacher, M. E., & Young, K. D. (2016). Dead-end intermediates in the enterobacterial common antigen pathway induce morphological defects in Escherichia coli by competing for undecaprenyl phosphate. *Mol Microbiol*, 100(1), 1-14. doi:10.1111/mmi.13284
10. Kawmura, T., Kimura, T., Yamamori, S., & Ito, E. (1978). Enzymatic Formation of Uridine Diphosphate N-Acetyl-D-mannosamine. Journal of Biological Chemistry, 253(10), 3595-3601.

11. Soldo, B., Lazarevic, V., Pooley, H. M., & Karamata, D. (2002). Characterization of a Bacillus subtilis Thermosensitive Teichoic Acid-Deficient Mutant: Gene mnaA (yvyH) Encodes the UDP-N-Acetylglucosamine 2-Epimerase. Journal of Bacteriology, 184(15), 4316-4320. doi:10.1128/jb.184.15.4316-4320.2002

12. Sala, R., Morgan, P., & Tanner, M. (1996). Enzymatic Formation and Release of a Stable Glycal Intermediate: The Mechanism of the Reaction Catalyzed by UDP-N-Acetylglucosamine-2-Epimerase. J. Am. Chem. Soc., 118, 3033-3034.

13. Kawamura, T., Ishimoto, N., & Ito, E. (1979). Enzymatic synthesis of uridine diphosphate N-acetyl-D-mannosaminuronic acid. *J Biol Chem*, 254(17), 8457-8465.

14. Kawamura, T., Ichihara, N., Ishimoto, N., & Ito, E. (1975). Biosynthesis of Uridine Dipohsphate N-Acetyl-D-Mannosaminuronic Acid from Urdine Diphosphate N-Acetyl-D-Glucosamine in *Escherichia coli*: Separation of Enzymes Responsible for Epimerization and Dehydrogenation. *Biochmical and Biophysical Research Communications.* ,66(4) 1506-1512.

15. Namboori, S. C., & Graham, D. E. (2008). Acetamido sugar biosynthesis in the Euryarchaea. *J Bacteriol*, 190(8), 2987-2996. doi:10.1128/JB.01970-07

16. Portoles, M., Kiser, K. B., Bhasin, N., Chan, K. H., & Lee, J. C. (2001). Staphylococcus aureus Cap5O has UDP-ManNAc dehydrogenase activity and is essential for capsule expression. *Infect Immun*, 69(2), 917-923. doi:10.1128/IAI.69.2.917-923.200

17. Palcic, M., & Sujino, K. (2001). Assays for Glycosyltransferases. *Trends in Glycoscience and Glycotechnology*, 13(72), 361-370.

18. Troutman, J. M., Erickson, K. M., Scott, P. M., Hazel, J. M., Martinez, C. D., & Dodbele, S. (2015). Tuning the production of variable length, fluorescent polyisoprenoids using surfactant- controlled enzymatic synthesis. *Biochemistry*, 54(18), 2817-2827. doi:10.1021/acs.biochem.5b00310

19. Sharma, S., Erickson, K. M., & Troutman, J. M. (2017). Complete Tetrasaccharide Repeat Unit Biosynthesis of the Immunomodulatory Bacteroides fragilis Capsular Polysaccharide A. *ACS Chemical Biology*, 12(1), 92-101. doi:10.1021/acschembio.6b00931

20. Scott, P. M., Erickson, K. M., & Troutman, J. M. (2019). Identification of the Functional Roles of Six Key Proteins in the Biosynthesis of *Enterobacteriaceae* Colanic Acid. *Biochemistry*. doi:10.1021/acs.biochem.9b00040

21. Warth, B., Siegwart, G., Lemmens, M., Krska, R., Adam, G., & Schuhmacher, R. (2015). Hydrophilic interaction liquid chromatography coupled with tandem mass spectrometry for the quantification of uridine diphosphate-glucose, uridine diphosphate-glucuronic acid, deoxynivalenol and its glucoside: In-house validation and application to wheat. *J Chromatogr A*, 1423, 183-189. doi:10.1016/j.chroma.2015.10.070

22. Ponten, Einar (2002). Zwitterion Chromatography (ZIC) *SeQuant*

23. Hesia, J., Van de Bittner, G., Chu, T., Potter, O., & Yin, H. (2018). Monitoring of Mammalian Cell Culture Media with HILIC LC/MS. *Agilent*.

24. Muthana, M. M., Qu, J., Li, Y., Zhang, L., Yu, H., Ding, L., . . . Chen, X. (2012). Efficient one-pot multienzyme synthesis of UDP-sugars using a promiscuous UDP-sugar pyrophosphorylase from *Bifidobacterium longum* (BLUSP). *Chem Commun*, 48(21), 2728-2730. doi:10.1039/c2cc17577k

25. Samuel, J., & Tanner, M. E. (2004). Active site mutants of the "non-hydrolyzing" UDP-N-acetylglucosamine 2-epimerase from *Escherichia coli*. *Biochim Biophys Acta*, 1700(1), 85-91. doi:10.1016/j.bbapap.2004.03.017

26. Napper, A. D., & Sivendran, S. (2011). Miniaturized High-Throughput Fluorescent Assay for Conversion of NAD(P)H to NAD(P). Curr Protoc Chem Biol, 3(2). doi:10.1002/9780470559277.ch100155

27. Krogh, A., Larsson, B., von Heijne, G., & Sonnhammer, E. L. (2001). Predicting transmembrane protein topology with a hidden Markov model: application to complete genomes. *J Mol Biol*, 305(3), 567-580. doi:10.1006/jmbi.2000.4315

28. Pradel, E., Parker, C. T., & Schnaitman, C. A. (1992). Structures of the rfaB, rfaI, rfaJ, and rfaS genes of Escherichia coli K-12 and their roles in assembly of the lipopolysaccharide core. *J Bacteriol*, 174(14), 4736-4745.

29. Rahman, A., Barr, K., & Rick, P. D. (2001). Identification of the structural gene for the TDP-Fuc4NAc:lipid II Fuc4NAc transferase involved in synthesis of enterobacterial common antigen in Escherichia coli K-12. *J Bacteriol, 183*(22), 6509-6516. doi:10.1128/JB.183.22.6509-6516.2001